Received <day> <Month>, <year>; | Revised <day> <Month>, <year>; | Accepted <day> <Month>, <year>

DOI: xxx/xxxx

ARTICLE TYPE

Dynamic damage identification using complex mode shapes

E. Lofrano[1,2] | A. Paolone[1] | G. Ruta[1,2]

[1]Structural and Geotechnical Engng., Univ. "La Sapienza", Rome, Italy
[2]Research group GNFM, National group of mathematical physics, Rome, Italy

Correspondence
*Egidio Lofrano, Structural and Geotechnical Engng. Univ. "La Sapienza", Via Eudossiana 18, Rome 00184, Italy.
Email: egidio.lofrano@uniroma1.it

Abstract

Damage, be it a material or a geometric degradation, modifies some features of the response foreseen by the original structural design. These variations, once the dependence onthe damage causing them is established, can be used for identification purposes. In the literature, vibration-based approaches usually compare some responses of linear elasticstructures with dissipative properties that are assumed proportional to the mass and stiffness measures. However, such an assumption is reasonable for new, undamaged structures,but can be unreliable in existing, potentially damaged structures, particularly for damages localised in narrow areas.

The eigenmodes of a proportionally damped system can be reduced to the real ones of the relevant ideal undamped system. On the other hand, non-proportional damping exhibits complex eigenmodes that cannot be reduced to those of the ideal, or of the proportionally damped, structure. Thus, we may assume the complexity of the eigenmodes as a measure of non-proportional damping, hence of damage. On this basis, some contributions in the literature verified the relationship among presence of damage and amount of complexity. Here we propose a perturbation approach and an objective function able to identify presence, location and amplitude of localised damages. A prototype naturally discrete structure with four degrees-of-freedom is chosen to test and show capability and accuracy of the proposed method.

KEYWORDS:
Dynamic identification; Modal complexity; Non-proportional damping; Perturbation approach; Structural damage identification; Vibration-based approach

1 | INTRODUCTION

In the last decades the investigations towards more refined and precise structural theories for design were accompanied by a rising interest for studies in structural identification and monitoring. Indeed, maintenance of existing structures in all fields of engineering asks for increasing attention, hence monitoring the present structures, identifying their health state, and foreseeing possible curing intervention attracts the interest of the scientific and technic community. However, structural identification is an inverse problem: the structural model (or an updating of the existing one) is the unknown to be searched, once some experimental measures of the structural response are at ease; the relevant analyses are often ill-conditioned problems. On the contrary, design is a direct problem: the loadings and the structural model are supposed to be known in advance (by technical instructions, state rulings, structural theories) and the unknown is some structural response (a characteristic displacement, the eigenproperties, and the like).

Due to its crucial importance for the structural health monitoring of existing structures, and the intrinsic scientific value of its inverse aspect, the scientific community is very interested in this topic, as shown by the number of international publications. We may refer to the literature review by Doebling *et al.*[1] for a first attempt of collecting and presenting an extensive state-of-the-art of that time. Another well-known contribution on this field is the paper by Farrar *et al.*[2], where vibration based damage detection is linked to the statistical distribution of response measurements and is described as a problem in statistical pattern recognition. An application to civil engineering is in Peeters *et al.*[3]: here various excitation sources, plus the effect of temperature on the change of eigenfrequencies, damping ratios and mode shapes are seen as indicators of potential damage. Another review of the state-of-the-art is the theme issue by Farrar & Worden[4], where international authors present an overview of the topic and some instances of research on sensors and detecting techniques and instruments, on static and vibration based identification techniques, on the new frontiers of health monitoring in civil, industrial and aerospace engineering. Another overview is in the monograph edited by Balageas *et al.*[5], where each chapter is devoted to the different aspects of structural health monitoring: an introductory overview to the problems and the methods, a thorough description of vibration based techniques, and extensive presentation of possible sensors, both contactless (optic) and attached to the structure (piezo-electric). The advantages of dynamic approaches were recently put into evidence in the monograph by Farrar & Worden[6], which provides a wide range introduction to the matter, together with essentials on deviations from linear structural response, probability and statistics, statistical pattern recognition, data normalisation. Further theoretical and practical discussions on the inverse methods for dynamic damage detection can be found in the work edited by Morassi & Vestroni[7].

Such analyses start from some assumptions on the nature of damage, either located in a narrow zone or diffused in a large area of the considered structural element. Limiting to localised damage, this is often thought as a local reduction of the resisting portion of the element (e.g., a reduction of the cross-section of a beam due to the apparition of a crack), or as a local fall of the properties of the material constituting the element (e.g., a decrement of the elastic moduli of the material due to thermal fatigue, corrosion, or similar causes). This leads to a local and sudden decrease of the stiffness properties that affect the structural response of the element, and, among others, the natural properties of free vibration. Such an approach is well established in the literature, and led to several contributions, among which we may quote Cawley & Adams[8] as a kind of starting point, to which we may add Christides & Barr[9] for a thorough formulation of a theory of Euler-Bernoulli beams affected by small, localised cracks. A first look at the identification problem as an inverse one for vibrating beams is found in Gladwell[10], and some instances of crack identification techniques for benchmark structural elements are found in Liang *et al.*[11,12]. More recent works are by Vestroni & Capecchi[13] and Sinha *et al.*[14]. One of the authors also contributed to the subject in the case of circular arches[15,16], with the crack thought as a lumped rotation spring separating two regular chunks. This is a standard approach in many of the quoted references, yet there are non-model based techniques, e.g. Lofrano *et al.*[17], which can be used for preliminary and/or complementary analyses.

Structural health monitoring is suitable in many engineering fields: we may quote Loh *et al.*[18] for vibration-based damage detection in such industrial apparatus as wind turbines; Rainieri *et al.*[19] for monitoring of civil structures and infrastructures in earthquake prone areas; Oregui *et al.*[20] for monitoring welded bolts by acceleration measurements; Diaferio & Sepe[21] and Antonacci *et al.*[22] on vibration measurements for damage detection in framed structures;and a very recent insight onto possible medical applications is in Ong *et al.*[23].

Undamaged civil, industrial, or aerospace framed structures can be described as proportionally damped systems, see the well-known monographs[24,25]: the physical quantity describing dissipation (damping) is supposed to be linearly related to the inertial and elastic properties. Then, the structure has real natural mode shapes in linear dynamics and, if it is naturally discrete, or made discrete by suitable assumptions, the mode shapes are lists of real quantities. In damaged structures the equations of motion in modal coordinates are coupled, and the mode shapes turn out to be described by complex quantities, especially when damages are concentrated in small areas. Thus, the complexity of the natural modes of a structure may be a measure of its state of damage, according to the results of the direct problem. Nevertheless, dissipative properties are rarely adopted to identify the presence of damage, or for structural health monitoring purposes. On this topic, Kawiecki[26] can be considered a pioneering work; another recently published proposal exploring this basic principle is by Iezzi *et al.*[27]. Anyway, these works are mainly focused on detecting the presence of damages. Some attempts dedicated to non-proportional damping identification, although not specifically related to damages, are reported in Link *et al.*[28], where a method based on model updating is applied to a finite element scheme.

This contribution considers the possibility of a perturbation approach for structural health monitoring and damage detection in framed structures with local damages. That is, a damaged configuration for a framed structure reducible to lumped characteristics (hence, to a system with a finite number of degrees of freedom) is seen as a small perturbation of the undamaged one. A direct

problem investigating the response of such modelled structures is investigated at first. We then propose a technique able to detect, quantify and localise structural damages. Through a perturbation scheme of the state-space formulation of the equations governing the dynamics of the structure, the amount of damages is evaluated through the minima of an objective function comparing the modal complexity of a) the measured and b) the analytical mode shapes. Some preliminary results of this method were recently presented by the authors at the EuroDyn 2017 conference[29]; here the technique is widely developed, tested, and thoroughly commented.

The paper has four parts: Section 2 presents the governing equations of a discrete mechanical system, which represents a framed structure with lumped characteristics; Section 3 illustrates the proposed method, basing on the perturbation scheme of Section 2; Section 4 presents the results of a numerical validation of the method on a benchmark structure, simulating a four-story civil frame exhibiting a localised damage; last, Section 5 points out the main conclusions and puts forth some final remarks.

2 | GOVERNING EQUATIONS

2.1 | Standard dynamic analysis

If dissipative properties are neglected, the free vibration of discrete or discretised linear mechanical system with n configuration descriptors (or degrees of freedom) is ruled by

$$\mathbf{M}\ddot{\mathbf{u}}(t) + \mathbf{K}\mathbf{u}(t) = \mathbf{0} \tag{1}$$

where the linearity of the system can be seen as a general application of the 'small-motions assumption'. Eq. (1) is differential, of second order with respect to the time t; $\mathbf{M}$ and $\mathbf{K}$ are the $n \times n$ mass and stiffness matrices of the structure, respectively, and $\mathbf{u}(t)$ is the list of the n generalised displacement components. Mass and stiffness are features of the system independent of time; the only time-dependent physical quantity is the list $\mathbf{u}$, describing the evolution of the configuration descriptors of the system.

Natural vibration about an equilibrium state is represented by harmonic time variation of the configuration descriptors

$$\mathbf{u}(t) = \mathbf{U}e^{-\imath\omega t}, \quad \imath := \sqrt{-1} \tag{2}$$

This separation of spatial and time-dependent quantities turns Eq. (1) into the non-standard eigenvalue problem

$$\left(\mathbf{K} - \omega^2\mathbf{M}\right)\mathbf{U} = \mathbf{0} \tag{3}$$

In 'stable' structural systems (i.e., with real, symmetric and positive definite mass and stiffness matrices), Eq. (3) is satisfied by a set of pairs of real eigenvalues and eigenvectors $(\omega_i^2, \mathbf{U}_i)$, $i = 1, 2, \dots, n$; where $\omega_i, \mathbf{U}_i$ represent the $i-$th natural angular frequency and mode shape, respectively, of the considered discrete mechanical system.

The simplest constitutive law for the dissipative actions ruling the energy loss assumes them proportional to the time rate of the configuration descriptors (viscous damping). Then, Eq. (1) must be updated and turns into

$$\mathbf{M}\ddot{\mathbf{u}}(t) + \mathbf{C}\dot{\mathbf{u}}(t) + \mathbf{K}\mathbf{u}(t) = \mathbf{0} \tag{4}$$

where $\mathbf{C}$ is the $n \times n$ matrix listing the damping coefficients of the system. In the literature on structural mechanics[24,25] it is commonly accepted that new (or, better, undamaged) structural systems have damping coefficients that might be assumed as directly related to the inertial and elastic coefficients of the structure through the Caughey series[30]

$$\mathbf{C} = \mathbf{M}\sum_{p=0}^{n-1} a_p \left(\mathbf{M}^{-1}\mathbf{K}\right)^p \tag{5}$$

where a_p are suitable coefficients, determined by experimental measures or fixing the so-called damping ratios

$$\xi_i = \frac{\mathbf{U}_i^\top \mathbf{C}\mathbf{U}_i}{2\omega_i \mathbf{U}_i^\top \mathbf{M}\mathbf{U}_i}, \quad \xi_i = \frac{1}{2\omega_i}\sum_{p=0}^{n-1} a_p \omega_i^{2p} \tag{6}$$

where Eq. $(6)_2$ derives from Eq. (5). If Eq. (5) holds, damping is said to be proportional, and it is easy to show that vibration can be decomposed along the same eigenvectors (mode shapes) $\mathbf{U}_i$ of the undamped case in Eq. (1).

On the other hand, when the damping matrix $\mathbf{C}$ does not satisfy Eq. (5), i.e., when the system is non-proportionally damped, Eq. (2) does not represent the natural modes of the considered system any more[24,25]. Thus, this standard analysis cannot describe damped structural dynamics, and a state-space formulation is needed, as follows.

2.2 | State-space formulation

The space state of a mechanical system is given by its configuration descriptors and their ratios with respect to time; that is, position and velocity can uniquely describe the response of the system. If we pose

$$\mathbf{z}(t) = \begin{bmatrix} \mathbf{u}(t) \\ \dot{\mathbf{u}}(t) \end{bmatrix}, \quad \mathbf{A} = \begin{bmatrix} \mathbf{C} & \mathbf{M} \\ \mathbf{M} & \mathbf{0} \end{bmatrix}, \quad \mathbf{B} = \begin{bmatrix} \mathbf{K} & \mathbf{0} \\ \mathbf{0} & -\mathbf{M} \end{bmatrix}, \tag{7}$$

the second order differential system in Eq. (4) is turned into a system of two sets of first order differential equations, and the free vibration of a non-proportionally damped mechanical system is governed by

$$\mathbf{A}\dot{\mathbf{z}}(t) + \mathbf{B}\mathbf{z}(t) = \mathbf{0} \tag{8}$$

A more general separation of space and state variables than that in Eq. (2) yields a more general eigenvalue problem

$$\mathbf{z}(t) = \mathbf{Z}e^{-\lambda t} \Rightarrow (\mathbf{B} - \lambda\mathbf{A})\mathbf{Z} = \mathbf{0} \tag{9}$$

where the pairs $(\lambda_i, \mathbf{Z}_i),\ i = 1, 2, \dots, 2n$ are the eigensolutions of the structure in terms of state-space variables. Under the same assumptions of Sub-section 2.1, $\mathbf{A}, \mathbf{B}$ are $2n \times 2n$ real, symmetric, non-positive definite matrices that admit complex conjugate couples of eigenpairs $(i = 1, 2, \dots, n)$

$$\begin{cases} \lambda_i = \xi_i\omega_i + \imath\omega_i\sqrt{1-\xi_i} \\ \lambda_{n+i} = \xi_i\omega_i - \imath\omega_i\sqrt{1-\xi_i} \end{cases} \qquad \begin{cases} \mathbf{Z}_i = \begin{bmatrix} \mathbf{U}_i \\ \lambda_i\mathbf{U}_i \end{bmatrix}, \quad \mathbf{U}_i \in \mathbb{C}^{n\times 1} \\ \mathbf{Z}_{n+i} = Re(\mathbf{Z}_i) - \imath Im(\mathbf{Z}_i) \end{cases} \tag{10}$$

Here, according to the notation of Sub-section 2.1, ω_i is the $i-$th natural angular frequency, ξ_i the $i-$th damping ratio, and the $\mathbf{U}_i$ list n quantities describing the mode shapes of vibration. At a first glance, things do not change much with respect to proportionally damped structures; basically, the same mode shapes $\mathbf{U}_i$, which were lists of real quantities in the standard dynamic analysis, become lists of complex numbers, representing out-of-phase vibration.

The dynamics of a proportionally damped mechanical system may also be described by state-space variables. The $i-$th natural angular frequency ω_i and $i-$th damping ratio ξ_i then coincide with those given by Eqs. (3), Eq. (6), respectively, and the natural modes are lists of complex numbers. This complexity is actually fictitious, sometimes labelled as 'dummy'. Indeed, the components of the natural modes of proportionally damped structures lie on straight segment of the real line in standard analysis, which is simply rotated in Gauss' complex plane in state-space analysis; this derives from the natural modes being independent of the analysis for their description. Thus, it is apparent that such complexity may be removed losing no information on the dynamics of the structure. On the contrary, in non-proportionally damped structures Eqs. (3), (6) do not hold, and the complexity of the natural modes cannot be eliminated, since it is intrinsic in the physics of the system. This dispersion of the complex components of the natural modes in the state-space description may be used to identify and evaluate the amount of non-proportional damping.

2.3 | Removing dummy complexity

The difference among the mode shapes of proportionally and non-proportionally damped structures is strictly related to the possibility of removing the dummy, or fictitious, complexity. To do that, we recall Liu's rotation[31], which rotates the straight line representing the best linear fit of the mode shape in the complex plane, and makes the real part of the mode a maximum and the imaginary part a minimum.

Liu's rotation of the i-th complex mode shape $\mathbf{U}_i$ given by the eigenvalue problem in Eq. (9) is highlighted by adding the subscript L, and described by the transformation

$$\mathbf{U}_{i,L} = \tilde{\mathbf{U}}_i e^{(-i\theta_i)}, \quad \tilde{\mathbf{U}}_i = \frac{\mathbf{U}_i}{U_{i,max}} e^{(\frac{i\pi}{4})} \tag{11}$$

with $U_{i,max}$ the maximum component of $\mathbf{U}_i$, and

$$\theta_i = \arctan\left(\frac{Re(\tilde{\mathbf{U}}_i)^T Im(\tilde{\mathbf{U}}_i)}{Re(\tilde{\mathbf{U}}_i)^T Re(\tilde{\mathbf{U}}_i)}\right) \tag{12}$$

The procedure is: by Eq. (11), the mode shape $\mathbf{U}_i$ is placed in the complex plane about a straight line through the origin at a counterclockwise angle of $\pi/4$ with respect to the real axis, yielding $\tilde{\mathbf{U}}_i$. The ratio $\mathbf{U}_i/U_{i,max}$ assures that each k-th component $(\tilde{U}_i)_k$ of $\tilde{\mathbf{U}}_i$ is such that $|\ (\tilde{U}_i)_k\ | \leq 1$, having normalised with respect to the component with maximum amplitude. Then, $\mathbf{U}_{i,L}$ is

obtained by rotating $\tilde{\mathbf{U}}_i$ in the complex plane by the clockwise angle θ_i in Eq. (12), which is the slope of the straight line through the origin of the complex plane that best fits (according to minimum squares) the dispersion of the components of $\tilde{\mathbf{U}}_i$.

To sum up, we have that (see also the scheme in Figure 1):

a. for undamped systems, Liu's rotation turns the straight segments, onto which the components of natural modes lie, by a right angle; since the modes obtained by state space dynamic analysis are purely imaginary, Liu's rotation brings them onto the real axis, and makes them coincide with those obtained by standard dynamic analysis;

b. for proportionally damped systems, the natural modes obtained by state space dynamic analysis are complex, but after Liu's rotation they become real and coincide with the real ones that would be obtained for zero damping;

c. for non-proportionally damped systems, the natural modes obtained by state space dynamic analysis are complex, but only part of this complexity is dummy; Liu's rotation superposes the best linear fit of the natural modes onto the real axis in the complex plane, making the real part of the modes a maximum and the imaginary part a minimum.

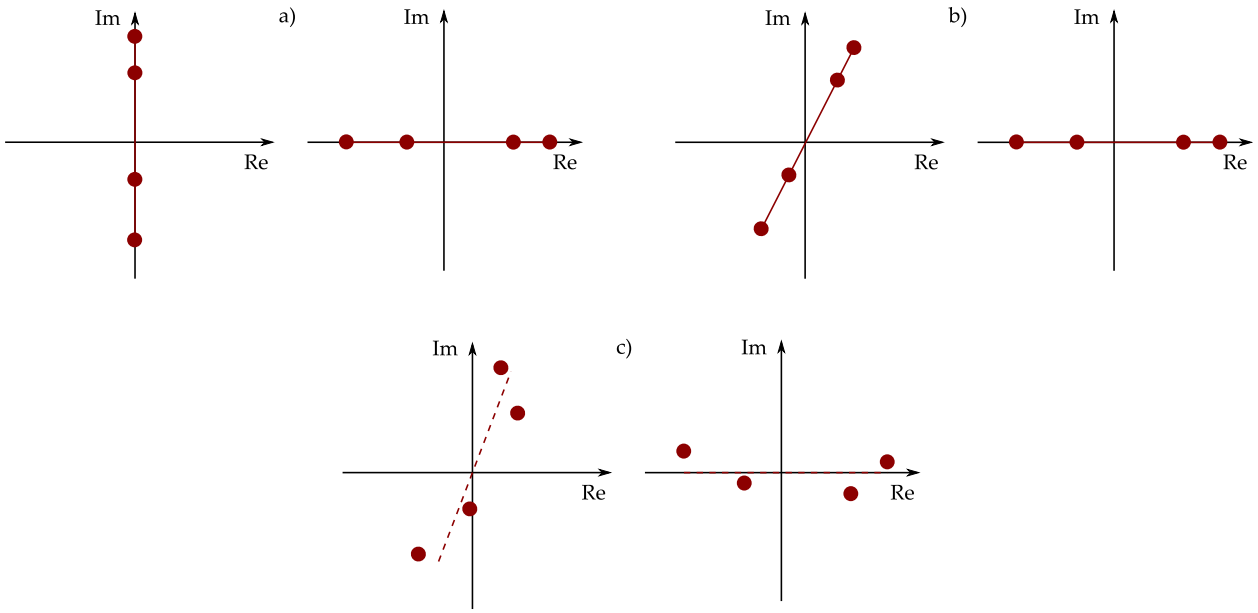

FIGURE 1 Components of mode shapes by state space analysis (left) and after Liu's rotation (right) for systems: undamped (a), proportionally damped (b), non-proportionally damped (c).

2.4 | Modal complexity for damage detection

Modal testing attracted the scientific community from the 1980s, concurrently with the rapid developments of computers and measuring instruments, see, e.g., Ewins[32]. In the vast literature that followed, undamped or classically damped mechanical systems were mainly analyzed, consequently neglecting the appearance of complex mode shapes. These approaches can be motivated by a simple assumption: the real part of the eigenmodes is related to the mass and stiffness distributions in the structure, whereas the complex part can be caused by several effects such as non-proportional damping, non-linear behavior, aerodynamic damping, gyroscopic effects, and poor test conditions (synchronization problems, low signal-to-noise ratios, weakly excited modes, etc.)[33], the magnitudes of which are generally limited in usual applications.

This objective difficulty in detecting the sources of complexification makes applications on large structures usually require specific modal complexity checks before the final clustering of structural modes[34]. At the same time, modal complexity cannot be always neglected (for instance, when external dissipators are inserted into structures); in these cases, a complex formulation must be suitably adopted to get the relevant outcomes[35,36].

In this work we base on a peculiar meaning of damage. Undamaged structures meet the assumption of proportional damping: as a result, their mode shapes are real. The onset of small, localised structural damages implies a loss of stiffness and an increase of dissipation with respect to the undamaged situation; on the other hand, except for very special cases, the variation of mass due to damage is usually negligible. Therefore, in general, damaged structures behave as non-proportionally damped systems, and exhibit complex mode shapes; the magnitude of their complex nature, once removed its fictitious part, can be assumed as a measure of damage.

To this aim, the amount of complexity of mode shapes is evaluated via a non-negative scalar function (a sort of norm) allowing to follow the damage evolution path. Resorting to the results in Iezzi *et al.*[27], for discrete n-degrees-of-freedom systems the following complexity indexes $I_h,\ h = 1, 2, \dots, 5$ are eligible and effective for localized damage ($|\bullet|$ and $\|\bullet\|$ stand for absolute value and Euclidean norm, respectively):

1. modal polygons[37]

$$I_1 = \sum_{i=1}^{n} \frac{A_i}{nA_{max}}, \quad A_{max} = n\cos\left(\frac{\pi}{n}\right)\sin\left(\frac{\pi}{n}\right) \tag{13}$$

where A_i is the area enclosed by the polygon representing the modal components of $\mathbf{U}_{i,L}$ in the complex plane, whereas A_{max} is the maximum potential area of modal polygons;

2. phase differences[37]

$$I_2 = \sum_{i=1}^{n} \frac{\phi_{i,max} - \phi_{i,min}}{n\pi} \tag{14}$$

with ϕ_i the phase angles of the displacement normalised i-th mode, and subscripts denoting maximum and minimum value; the ϕ_i span the first quadrant of Gauss' plane and are the phase angles of the vectors $|\ Re(\mathbf{U}_{i,L})\ | + \imath\ |\ Im(\mathbf{U}_{i,L})\ |$;

3. modal collinearity[31]

$$I_3 = \sum_{i=1}^{n} \frac{1}{n} \frac{|\ Re(\mathbf{U}_{i,L})^T Im(\mathbf{U}_{i,L})\ |}{\sqrt{[Re(\mathbf{U}_{i,L})^T Re(\mathbf{U}_{i,L})][Im(\mathbf{U}_{i,L})^T Im(\mathbf{U}_{i,L})]}} \tag{15}$$

with $\mathbf{U}_{i,L}$ the i-th complex natural mode after Liu's rotation;

4. average of the imaginary parts of the natural modes[31]

$$I_4 = \sum_{i=1}^{n}\sum_{k=1}^{n} \frac{|\ Im((U_{i,L})_k)\ |}{n^2} \tag{16}$$

where $(U_{i,L})_k$ is the k-th component of $\mathbf{U}_{i,L}$;

5. weight of the imaginary part of the natural modes[38]

$$I_5 = \sum_{i=1}^{n} \frac{\|Im(\mathbf{U}_{i,L})\|}{n\|\mathbf{U}_i\|} \tag{17}$$

The I_h are always positive and go to zero when damping is proportional or null. To ensure damage identifiability, the I_h shall be damage sensitive, rather pseudo-linear, and monotonically increasing with the damage evolution; we discuss these requirements in the application we deal with.

3 | DAMAGE AS A PERTURBATION

Damages are often 'small' variations of the physical properties of the intact system; thence, a perturbation of its response represents the effect of damage, see Lofrano emphet al.[39,40] for discrete undamped and classically damped dynamical systems, respectively. Analytically, the amount of damage is measured by a 'small' scalar parameter ϵ, as in many perturbation approaches: a load in buckling and post-buckling analysis, as in Pignataro *et al.*[41,42]; a length scale parameter in Ruta *et al.*[43,44]; instances in dynamics are inNayfeh's monograph[45]; recent developments in a non-linear framework are in Lacarbonara *et al.*[46]. In dynamics discrete or discretised systems are more often adopted, since vibrating continua, see Lofrano *et al.*[47], require additional hypotheses on the number of mode shapes to be considered in the evaluation of perturbation terms.

We present the direct problem, and determine the response variation due to damage by a perturbation approach. Then, in the inverse problem we use (some of) the damage indicators I_h in order to detect damage.

3.1 | Direct problem

We pose that a discrete system has dynamic behaviour depending with sufficient regularity on a small parameter $\varepsilon \ll 1$ expressing the amount of damage. Then, it is natural that all state space descriptors also regularly depend on ε

$$\left(\mathbf{M}, \mathbf{C}, \mathbf{K}, \lambda_i, \mathbf{Z}_i\right) = \left(\mathbf{M}(\varepsilon), \mathbf{C}(\varepsilon), \mathbf{K}(\varepsilon), \lambda_i(\varepsilon)\mathbf{Z}_i(\varepsilon)\right) \tag{18}$$

The sensitivity analysis of the eigensolutions with respect to the damage indicator is developed following a perturbation approach: due to the supposed regularity of the functions in Eq. (18), one can perform a formal ε-power series expansion of the physical quantities of the system around $\varepsilon = 0$

$$\begin{cases} \mathbf{M}(\varepsilon) = \mathbf{M}_0 + \varepsilon\mathbf{M}_1 + \varepsilon^2\mathbf{M}_2 + \dots \\ \mathbf{C}(\varepsilon) = \mathbf{C}_0 + \varepsilon\mathbf{C}_1 + \varepsilon^2\mathbf{C}_2 + \dots \\ \mathbf{K}(\varepsilon) = \mathbf{K}_0 + \varepsilon\mathbf{K}_1 + \varepsilon^2\mathbf{K}_2 + \dots \end{cases} \tag{19}$$

In Eq. (19) the following positions hold

$$(\mathbf{M}_j, \mathbf{C}_j, \mathbf{K}_j) = \frac{1}{j!}\frac{\mathrm{d}^j(\mathbf{M}(\varepsilon), \mathbf{C}(\varepsilon), \mathbf{K}(\varepsilon))}{\mathrm{d}\varepsilon^j}\bigg|_{\varepsilon=0} \tag{20}$$

The literature considers two types of dynamic systems, *non-nilpotent* (non-defective) and *nilpotent* (defective) to guarantee solvability of eigenvalue problems by perturbation schemes. Systems of the first type see algebraic and geometric multiplicity coincide (each eigenvalue with multiplicity r generates an eigenspace of dimension r); the remaining systems belong to the second type. In[48] it is rigorously shown that non-nilpotent systems admit solution as a perturbation series of integer powers of the 'small' parameter (Taylor series); on the contrary, fractional powers (Puiseux series) are needed for nilpotent systems[49].

The dynamic systems considered here are ruled by symmetric operators (see Eq. $(9)_2$) that cannot be defective; then, eigensolutions can be expanded in a formal powers series of ε with integer exponents, i.e.,

$$\begin{cases} \lambda_i = \lambda_{0i} + \varepsilon\lambda_{1i} + \varepsilon^2\lambda_{2i} + \dots \\ \mathbf{Z}_i = \mathbf{Z}_{0i} + \varepsilon\mathbf{Z}_{1i} + \varepsilon^2\mathbf{Z}_{2i} + \dots \end{cases} \tag{21}$$

The perturbation approach in Eqs. (19–21) leads to

$$\begin{gathered} [\mathbf{B}_0 + \varepsilon\mathbf{B}_1 + \varepsilon^2\mathbf{B}_2 + \dots - (\lambda_{0i} + \varepsilon\lambda_{1i} + \varepsilon^2\lambda_{2i} + \dots)(\mathbf{A}_0 + \varepsilon\mathbf{A}_1 + \varepsilon^2\mathbf{A}_2 + \dots)](\mathbf{Z}_{0i} + \varepsilon\mathbf{Z}_{1i} + \varepsilon^2\mathbf{Z}_{2i} + \dots) = \mathbf{0} \\ \mathbf{A}_k = \begin{bmatrix} \mathbf{C}_k & \mathbf{M}_k \\ \mathbf{M}_k & \mathbf{0} \end{bmatrix}, \quad \mathbf{B}_k = \begin{bmatrix} \mathbf{K}_k & \mathbf{0} \\ \mathbf{0} & -\mathbf{M}_k \end{bmatrix}, \quad k = 0, 1, 2 \dots \end{gathered} \tag{22}$$

The problem in Eq. (22) can be re-arranged into a collection of eigenvalue problems, the solutions of which have the form in Eq. (21), which we arrest at the second order, i.e., within an error $o(\varepsilon^2)$. As common in perturbation approaches, the eigenproperties of order 1 and 2 can be written in closed form, starting from the 0-th order solution $(\lambda_0, \mathbf{Z}_0)$.

Balancing the power of ε, after some manipulations and simplifications we obtain

$$\begin{cases} \lambda_{1i} = \dfrac{\mathbf{Z}_{0i}^\top(\mathbf{B}_1 - \lambda_{0i}\mathbf{A}_1)\mathbf{Z}_{0i}}{\mathbf{Z}_{0i}^\top\mathbf{A}_0\mathbf{Z}_{0i}} \\ \mathbf{Z}_{1i} = \alpha_{ii}\mathbf{Z}_{0i} + \displaystyle\sum_{\substack{j=1 \\ j\neq i}}^{2n} \frac{\mathbf{Z}_{0j}^\top(\mathbf{B}_1 - \lambda_{0i}\mathbf{A}_1)\mathbf{Z}_{0i}}{(\lambda_{0i} - \lambda_{0j})\mathbf{Z}_{0j}^\top\mathbf{A}_0\mathbf{Z}_{0j}}\mathbf{Z}_{0j} \end{cases} \tag{23}$$

at order 1, while at order 2 we have

$$\begin{cases} \lambda_{2i} = \dfrac{\mathbf{Z}_{0i}^\top(\mathbf{B}_1 - \lambda_{0i}\mathbf{A}_1 - \lambda_{1i}\mathbf{A}_0)\mathbf{Z}_{1i}}{\mathbf{Z}_{0i}^\top\mathbf{A}_0\mathbf{Z}_{0i}} + \dfrac{\mathbf{Z}_{0i}^\top(\mathbf{B}_2 - \lambda_{0i}\mathbf{A}_2 - \lambda_{1i}\mathbf{A}_1)\mathbf{Z}_{0i}}{\mathbf{Z}_{0i}^\top\mathbf{A}_0\mathbf{Z}_{0i}} \\ \mathbf{Z}_{2i} = \beta_{ii}\mathbf{Z}_{0i} + \displaystyle\sum_{\substack{j=1 \\ j\neq i}}^{2n} \left(\frac{\mathbf{Z}_{0j}^\top(\mathbf{B}_1 - \lambda_{0i}\mathbf{A}_1 - \lambda_{1i}\mathbf{A}_0)\mathbf{Z}_{1i}}{(\lambda_{0i} - \lambda_{0j})\mathbf{Z}_{0j}^\top\mathbf{A}_0\mathbf{Z}_{0j}} + \frac{\mathbf{Z}_{0j}^\top(\mathbf{B}_2 - \lambda_{0i}\mathbf{A}_2 - \lambda_{1i}\mathbf{A}_1)\mathbf{Z}_{0i}}{(\lambda_{0i} - \lambda_{0j})\mathbf{Z}_{0j}^\top\mathbf{A}_0\mathbf{Z}_{0j}} \right)\mathbf{Z}_{0j} \end{cases} \tag{24}$$

(details are in Appendix); α_{ii}, β_{ii} are undetermined amplification parameters. According to this technique, the 0-th order solution describes the undamaged state of the system, while the terms of order 1 and 2 in Eqs. (23), (24) are small detachments from

the undamaged state and express closed-form solutions of the dynamics of damaged structures. Remark that this solution suits non-resonant systems (like the framed structures we investigate), for which $|\lambda_{0i} - \lambda_{0j}| \nrightarrow 0 \; \forall i \neq j$; resonant or nearly-resonant (non-nilpotent) systems require other well-suited techniques[50].

3.2 | Inverse problem

We propose an identification technique requiring three steps:
1. experimental modal complexity indexes are chosen and evaluated basing on actual measures, Figure 2;

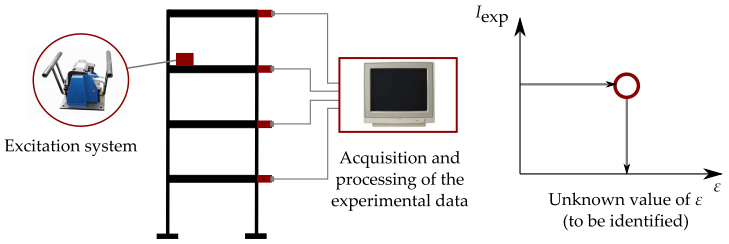

FIGURE 2 First step of identification.

2. assume to know the matrices $\mathbf{M}_0, \mathbf{C}_0, \mathbf{K}_0$ of the undamaged system; then, the perturbation approach in Eqs. (19–21) provides a numerical estimate of the chosen modal complexity indexes in function of the position and magnitude of the damage. Supposing that the damage is located at different positions within the structure provides a series of candidate damaged structural models $\mathcal{M}_h$, each characterised by the perturbation quantities $(\lambda^h_{1i}, \mathbf{Z}^h_{1i})$ and $(\lambda^h_{2i}, \mathbf{Z}^h_{2i})$. The magnitude of the damage is the value of ε scaling the eigensolutions according to the formal expansion in Eq. (21). Then, for each $\mathcal{M}_h$ one may find a function providing the chosen modal complexity indexes I_{pert} versus the amount of damage ε, Figure 3_a. The actual value of the chosen modal complexity indexes I_{exp} lets some candidate model be eliminated, while the other $\mathcal{M}_h$ yield the same value I_{exp} for different levels of damage $\tilde{\varepsilon}_h$, see Figure 3_b;

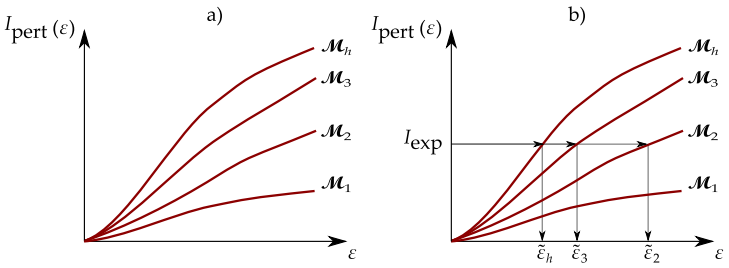

FIGURE 3 Second step of identification: a) complexity indexes vs. damage parameter for various candidates; b) possible amounts of damage for various candidates.

3. the candidate model best representing the actual damage location is found by minimising the objective function (OF)

$$\text{OF}(\mathcal{M}_h) = \sum_{i=1}^{n} \left(1 - \sqrt{\text{MAC}(\mathbf{U}^h_{i,L}, \tilde{\mathbf{U}}_{i,L})}\right)^2 \tag{25}$$

In Eq. (25) $\tilde{\mathbf{U}}_{i,L}$ is the measured i-th mode shape after Liu's rotation, $\mathbf{U}^h_{i,L}$ is the same mode given by the h-th candidate model $\mathcal{M}_h$ (setting the damage parameter equal to $\tilde{\varepsilon}_h$), and MAC (*Modal Assurance Criterion*) is

$$\text{MAC}(\mathbf{a}, \mathbf{b}) = \frac{|\, \mathbf{a}^\top \mathbf{b} \,|^2}{(\mathbf{a}^\top \mathbf{a})(\mathbf{b}^\top \mathbf{b})} \tag{26}$$

for any two vectors $\mathbf{a}, \mathbf{b}$. MAC was introduced in[51] to improve previous criteria, affected by error propagation in evaluating the matrices of the system. MAC is real, with values in $[0, 1]$: the first extremum indicates no correspondence between the considered vectors, the second a perfect correspondence; details are in[52]. Using MAC in the OF fits the scope of measuring the consistency of the actual (measured) mode shapes with the eigenvectors provided by the candidate modes $\mathcal{M}_h$, independent of the value of ε. The proposed OF uses Least Squares Method (LSM) and its global minimum provides the best candidate model, Figure 4_a, which in turn provides an estimate of the actual damage measure $\tilde{\varepsilon}_h$, Figure 3_b. Even neglecting all error sources, real (actual) and estimated (identified) damage differ: indeed, the truncation of the series expansion in the perturbation scheme cannot provide an exact sum. Within the limits of acceptability of this expansion, the higher its order, the smaller the deviation, i.e., the discrepancy is as small as ε, Figure 4_b.

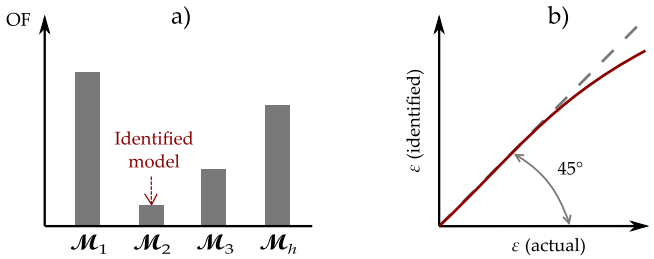

FIGURE 4 Third step of identification: a) best candidate model and b) truncation error.

By our experience, a second-order approach makes the truncation discrepancy negligible if $\varepsilon < 0.20$; if $\varepsilon > 0.20$, the technique should be applied carefully, since the solution is 'too far' from the generating one, and the results could be unreliable. Conversely, when $\varepsilon < 0.20$ the technique is suitable for detecting, quantifying and localising structural damages; these features classify our method at level 3 identification techniques according to Table 1.

TABLE 1 Levels of damage identification[53].

Level	Presence	Entity	Position	Remaining life
1	√	×	×	×
2	√	√	×	×
3	√	√	√	×
4	√	√	√	√

This flowchart looks reliable, fast and easy to apply, but some remarks are needed. First, the critical judgment of the personnel involved is crucial to limit the number of candidate models, i.e., the overall computational effort required by our proposal: roughly speaking, the number of $\mathcal{M}_h$ should be minimum. Furthermore, we posed to know $\mathbf{M}_0, \mathbf{C}_0, \mathbf{K}_0$ from a design analysis or a preliminary experimental campaign. In the latter case, the same approach presented here can be applied, considering ε a measure of the 'distance' from the actual matrices to the assumed ones. We also highlight how our approach admits an initial non-proportional damping matrix (that is, $\mathbf{C}_0$ does not meet Caughey rule in Eq. (5)); this fulfills the comparison criterion "assessment of damage requires a comparison between two system states" of the axiomatic theory on structural health monitoring, postulated by Worden *et al.*[54].

4 | NUMERICAL VALIDATION

We present a numerical validation of the reliability of our technique: its accuracy is actually strongly related to that of the experimental campaign (see the comments in Sub-section 2.4), remembering the computational aspects required to collect complex mode shapes[55]. To address this, we are planning a validation by lab experiments.

Consider a plane shear-type 4-story frame reduced to a discrete four degrees-of-freedom structure, see Figure 5. We assume $m = 1\text{kg},\ k = 1.8\text{kN/m}$ for mass and stiffness, to facilitate laboratory tests and to provide a modal model consistent with real steel framed structures.

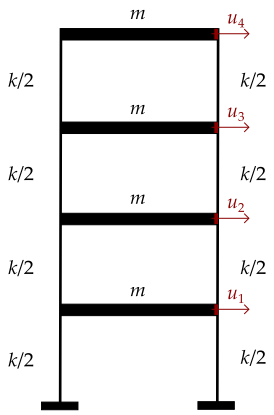

FIGURE 5 Structural model.

Describing motion by the absolute displacement $u_i, i = 1-4$ of each story[24] yields mass and stiffness matrices

$$\mathbf{M}_0 = \begin{bmatrix} m & 0 & 0 & 0 \\ 0 & m & 0 & 0 \\ 0 & 0 & m & 0 \\ 0 & 0 & 0 & m \end{bmatrix} = \text{diag}\left[m\right]_{4\times4} = \text{diag}\left[1\right]_{4\times4}\text{kg}, \quad \mathbf{K}_0 = \begin{bmatrix} 2k & -k & 0 & 0 \\ -k & 2k & -k & 0 \\ 0 & -k & 2k & -k \\ 0 & 0 & -k & k \end{bmatrix} = \begin{bmatrix} 3.6 & -1.8 & 0 & 0 \\ -1.8 & 3.6 & -1.8 & 0 \\ 0 & -1.8 & 3.6 & -1.8 \\ 0 & 0 & -1.8 & 1.8 \end{bmatrix} \frac{\text{kN}}{\text{m}}$$

The damping matrix $\mathbf{C}$ of the undamaged system is posed Rayleigh-like, i.e., proportional to mass and stiffness as

$$\mathbf{C}_0 = a_0\mathbf{M}_0 + a_1\mathbf{K}_0, \quad a_0 = 0.31501/\text{s},\ a_1 = 0.0003\text{s}$$

It is evident that Rayleigh damping is given by Eq. (5) when only the first two terms are retained in Caughey's series.

The natural properties of the undamaged structure may be found by standard libraries, since we deal with an usual and well-known, numerically well-treated eigenvalue problem, no matter whether in a standard or non-standard form. However, in this case the limited amount of degrees of freedom made it possible to develop a *in-house* code in a standard programming language; in addition, this helps, in a second step, to check the proposed identification procedure.

The natural modes of the undamaged structure and their placement in the complex plane are sketched in Figure 6, which consists of four distinct plots. One shows the shape of the natural modes in the plane of the structure, the other three show by coloured bullets the location of the numerical entries of the lists expressing the natural modes in Gauss' plane. On top right, we see that the natural modes all lie on the real axis after a standard dynamic analysis, since the considered structure is proportionally damped, see Sub-section 2.1. On top left, the same lists fill straight segments in the complex plane after a state-space analysis, according to the theory in Sub-section 2.1 for proportionally damped structures; the angles of Liu's rotation (see Sub-section 2.3) are pointed out. On bottom left, we see how Liu's rotation actually superposes the straight segments of the sub-figure top left onto the real axis, and makes them coincide with those in sub-figure top right. On bottom right, we see the shapes of the natural modes, exhibiting the symmetries expected from the discrete structure considered, with the relevant values of frequencies $f_i = \omega_i/(2\pi)$ and damping ratios ξ_i.

We now introduce a local damage for the considered structure, imagining it as a perturbation of the undamaged state. As already said, a local damage does not to alter the mass properties of a mechanical system, hence the mass matrix $\mathbf{M}(\varepsilon)$ remains

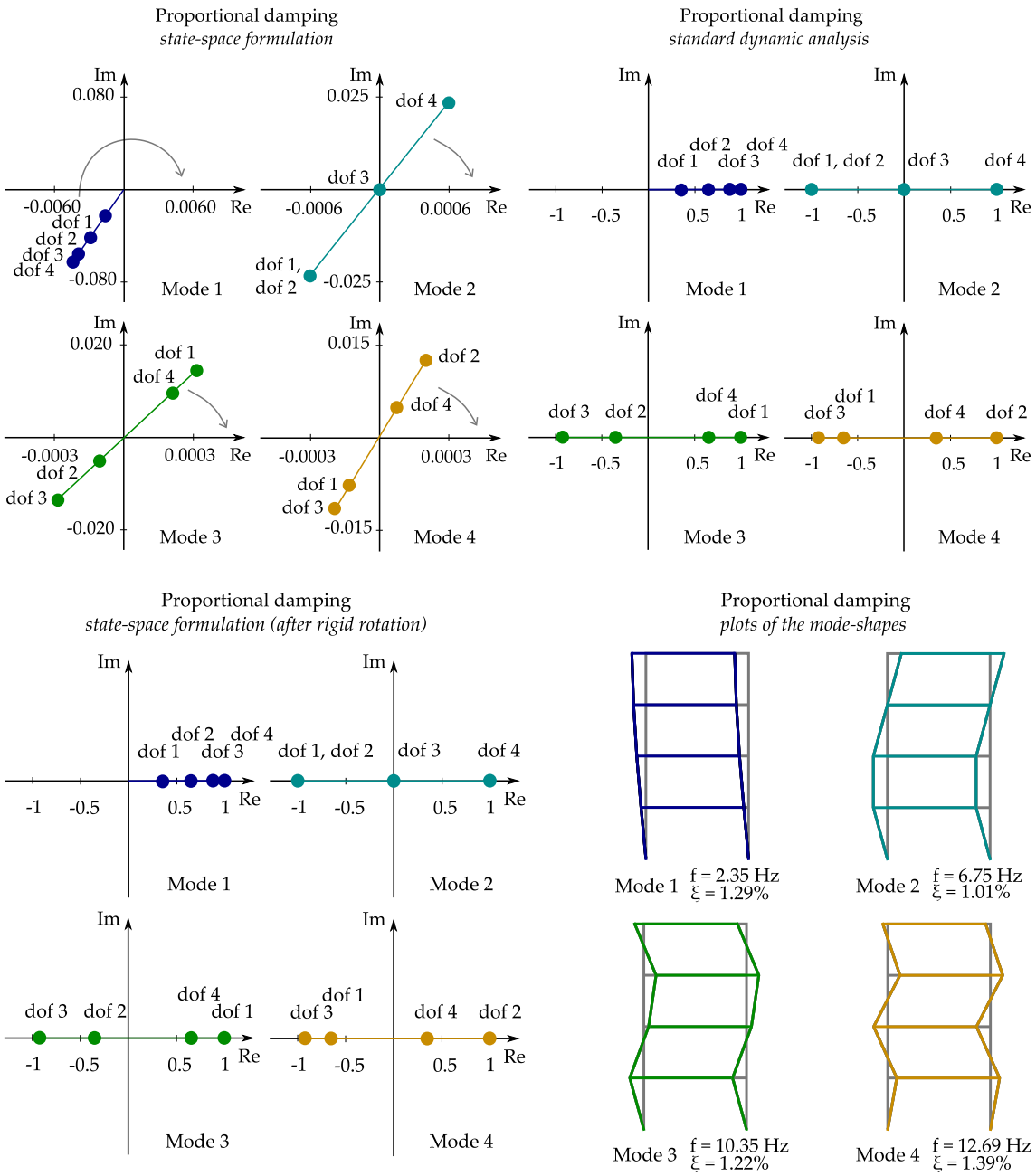

FIGURE 6 Natural mode shapes of the initial (undamaged) system.

unaffected by the perturbation scheme in Eq. (19); thus, in the simulations to validate the proposed procedure we assume

$$\mathbf{M}(\varepsilon) = \mathbf{M}_0$$

The damage is supposed 'small', located at the third floor; the parameter ε is imagined to act in three different ways:

1. ε affects the stiffness matrix $\mathbf{K}(\varepsilon)$;
2. ε affects the damping matrix $\mathbf{C}(\varepsilon)$;
3. ε affects both stiffness and damping $\mathbf{K}(\varepsilon), \mathbf{C}(\varepsilon)$.

In detail, in case 1 damage is simulated as a first-order variation of the undamaged matrix $\mathbf{K}_0$, consisting in a local reduction of magnitude εk of the stiffness at the third story. Thus, the global stiffness matrix of the damaged structure is

$$\mathbf{K}(\varepsilon) = \mathbf{K}_0 + \varepsilon k \begin{bmatrix} 0 & 0 & 0 & 0 \\ 0 & -1 & 1 & 0 \\ 0 & 1 & -1 & 0 \\ 0 & 0 & 0 & 0 \end{bmatrix}$$

In case 2, damage is simulated as a first-order variation of the undamaged matrix $\mathbf{C}_0$, consisting in a local increase of magnitude εc_3 of the damping coefficient at the third story. Thus, the damping matrix $\mathbf{C}$ of the damaged structure is

$$\mathbf{C}(\varepsilon) = \mathbf{C}_0 + \varepsilon c_3 \begin{bmatrix} 0 & 0 & 0 & 0 \\ 0 & 1 & -1 & 0 \\ 0 & -1 & 1 & 0 \\ 0 & 0 & 0 & 0 \end{bmatrix}$$

With no loss in generality, in the numerical simulations we adopt $c_3 = 25$Ns/m; following the notation in Sub-section 2.2, when $\varepsilon = 0.20$ (the reliability threshold indicated in Sub-section 3.2) this value of c_3 is able to increase the damping ratios ξ_i shown in Figure 6 from 1.29, 1.01, 1.22 and 1.39 % to 1.66, 2.96, 1.67 and 6.19 %, respectively.

In case 3, damage is simulated as a first-order variation of both the stiffness and damping matrices of the undamaged structure: it consists of both a reduction in stiffness of magnitude εk and an increase in damping of magnitude εc_3 at the third story. Since the mass matrix of the damaged system is assumed equal to that of the undamaged structure, these variations of stiffness and damping, either individual or cumulative, certainly lead to non-proportionally damping conditions, i.e., dissipation properties not matching Eq. (5). The three states of damage are sketched in Figure 7.

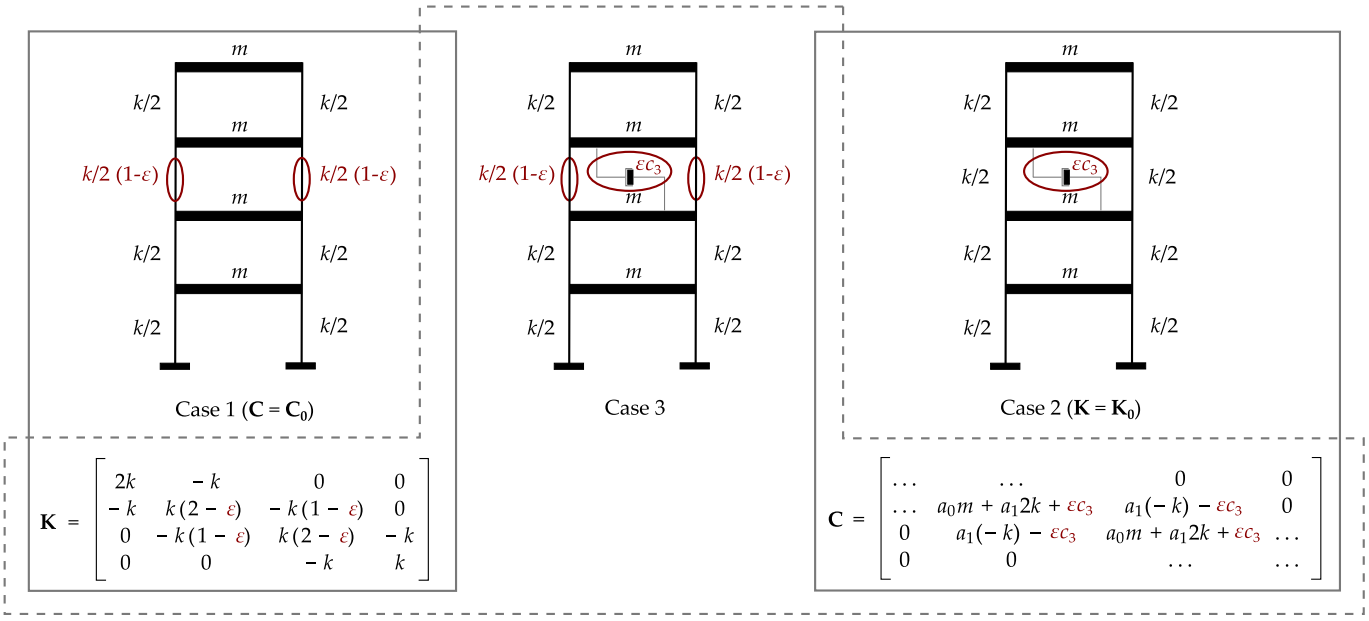

FIGURE 7 Damaged states: 1) (left) stiffness reduction; 2) (right) damping increase; 3) (middle) combination of 1) and 2).

4.1 | Sensitivity analysis of eigensolutions

We investigate the results of our *in-house* numerical code on the natural properties of the considered structure affected by the first damage state described (a first-order stiffness reduction at the third story). We limit to this since from the point of view of damage detection the key point is a thorough investigation of the response of the complexity indexes introduced in Section 2, to

choose to most predictive one for applications. Thus, we limit to show how our technique is able to follow the evolution of the natural properties with the growth of damage, and provide results both in accord with physics and suitable to be inserted into a procedure of damage identification for structural health monitoring.

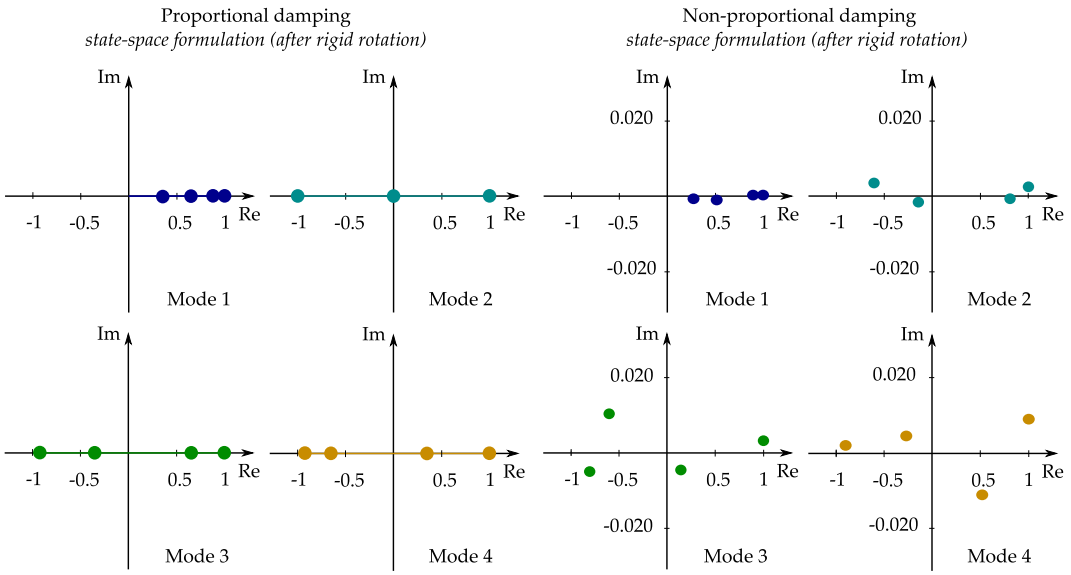

FIGURE 8 Real (left, $\varepsilon = 0$) and complex (right, $\varepsilon = 0.5$) mode shapes for the damage case 1.

By considering a reduction of stiffness amounting to $\varepsilon = 0.5$, the bullets describing the natural modes of the damaged system are in Figure 8 (right), and those for the undamaged structure are juxtaposed on the left, for the sake of a thorough comparison. The analysis is performed with respect to state-space variables, and the plots follow Liu's rotation, in order to normalise each mode with respect to its maximum component and minimise their imaginary part. We may check that all the modes of the undamaged structure are real, and those of the damaged structure exhibit an amount of complex properties (imaginary parts for all the entries of the lists providing the modes). In our application, moreover, complexification is more significant for faster oscillations (third and fourth mode), whereas it is less noticeable for slower ones (first and second mode). We believe that this result can be generalized and applied within the framework of optimal sensors placement; however, this topic belongs to a still ongoing investigation, beyond the scope of this paper.

Further insights for the direct problem are in Figures 9 and 10, which show exact solutions (ES) versus the 1^{st}- and 2^{nd}-order solutions provided by the perturbation approach (PA), both for the eigenvalues (i.e., the imaginary and real parts of eigenvalues of the dynamic problem) and the four components (with real and imaginary parts) of the fastest natural mode (i.e., the fourth mode shape of the dynamic problem) before Liu's rotation. The exact solutions are so defined since they are the eigensolutions of the complete problem expressed by Eq. 9, while the 1^{st}- and 2^{nd}-order solutions are provided by Eq. 21. The curves providing the so-called exact solutions are solid, the others are dashed.

In Figure 9 we see that the actual values of the real and imaginary parts of the eigenvalues and of their decrease ratio due to damage are very well approximated by the first-order perturbation approach if the 'small' parameter remains below 0.5. The first three values of the imaginary part (in increasing order) are approximated from above, the last and highest value from below; the opposite happens for the real part of the eigenvalues. However, we remark that in the range $0 \leq \varepsilon \leq 0.50$ the approximation is always very good, no matter which is the considered mode. On the other hand, the first-order approximated values of the real and imaginary parts of the components of the fastest mode shape practically coincide with the exact ones as long as $\varepsilon < 0.20$. After such value, the approximated values of the imaginary and real parts dominate the actual ones from above.

As to the second-order approximation, Figure 10 shows that both the real and the imaginary part of the eigenvalues are very well approximated by the perturbation approach up to $\varepsilon \approx 0.70$, approaching from below or above as the first-order solution. For the real and imaginary parts of the components of the fastest mode shape, however, the improvement gathered using a second-order approximation instead of a linear one is less notable, and a very good approximation requires again $\varepsilon < 0.20$. Beyond this

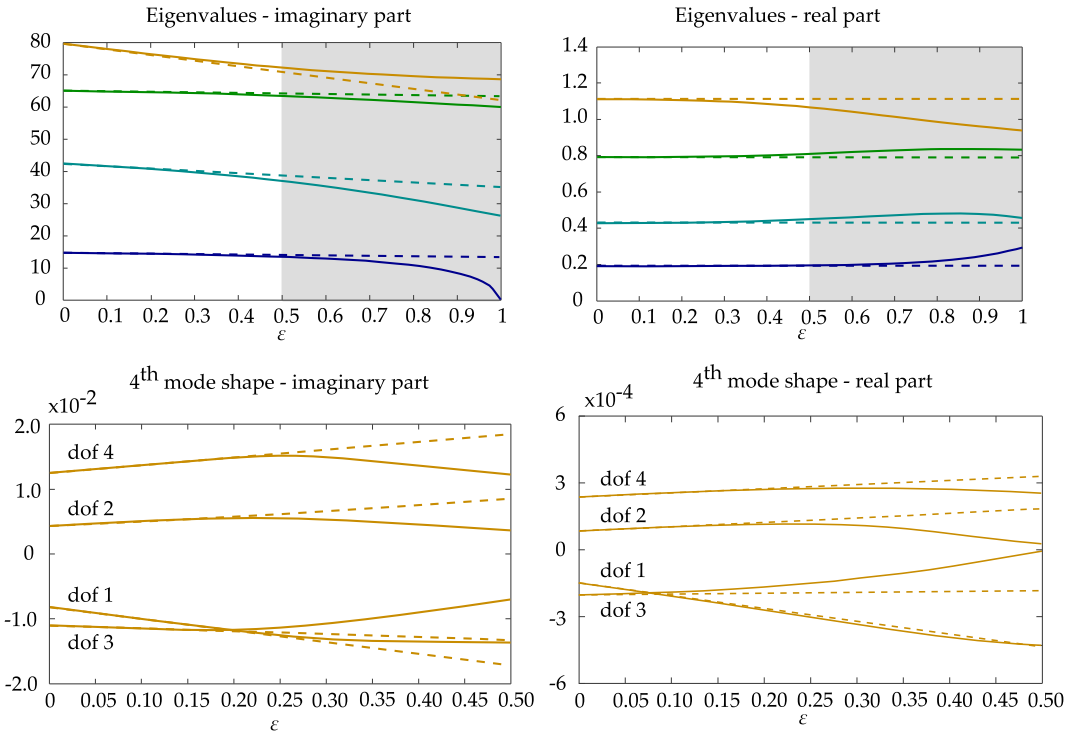

FIGURE 9 Complex eigensolutions (eigenvalues and fastest mode shape): case 1, first-order solution.

threshold, approximated values dominate the exact ones all from above, which may result in overestimating displacements; this has some importance in identification.

4.2 | Sensitivity analysis of complexity indexes

We investigate how the results for the eigenproperties of the damaged structure according to the exact approach in Eq. (9) and to the first- and second-order perturbation approximations provided by Eq. (21) affect the modal complexity indexes defined by Eqs. (13–17).

The index I_2 (Eq. (14)) can be misleading: the phase difference relates complexification only to the extrema of a mode, neglecting the other $n-2$ components. For instance, Figure 11_a shows one of our simulations (damage case 1, closest view in the range $0.20 \leq \varepsilon \leq 0.40$), where the ratio $(\phi_{i,max} - \phi_{i,min})/\pi$ mistakenly decreases for the second mode while damage increases. Figure 11_b shows the path of the relevant phase angles ϕ_i defined in Sub-section 2.4, that should be identically zero for undamped or proportionally damped systems. It is apparent that the bad performance of I_2 is related to the adoption of just the two extremal values. Then, from now on we do not explicitly evaluate I_2, and we show graphs on I_1, $I_3 - I_5$ in Figures 12, 13, and 14 for the damage cases 1,2, 3, respectively. As previously, solid lines represent the so-called exact solution, and dashed lines represent first- and second-order approximations.

Figure 12 shows that in the first damage case (stiffness reduction) the complexity indexes I_1, $I_3 - I_5$ are suitable to quantify the damage increase. All the approximated values lie below those provided by the exact solution, independent of the chosen index, and the approximation is quite good for low values of ε, then the first- and second-order paths detach sensibly from the actual ones, even though the second-order approach clearly improves the description of actual curves.

Figure 13 shows that also in the second damage case (damping increase) the complexity indexes I_1, $I_3 - I_5$ appear eligible for damage detection. However, approximated values of index I_1 are not satisfying, since they are sometimes higher, then lower than the exact ones, which is not desirable in identification procedures. On the contrary, the actual curves of the indexes I_3 to I_5 are always enclosed between the approximated ones of the perturbation approach, and this monotonicity is important in the applications. As in the previous case, for low values of ε (i.e., a small amount of damage), the three curves almost coincide; moreover, in this case even a first-order perturbation procedure suffices to have a very reliable complexity index.

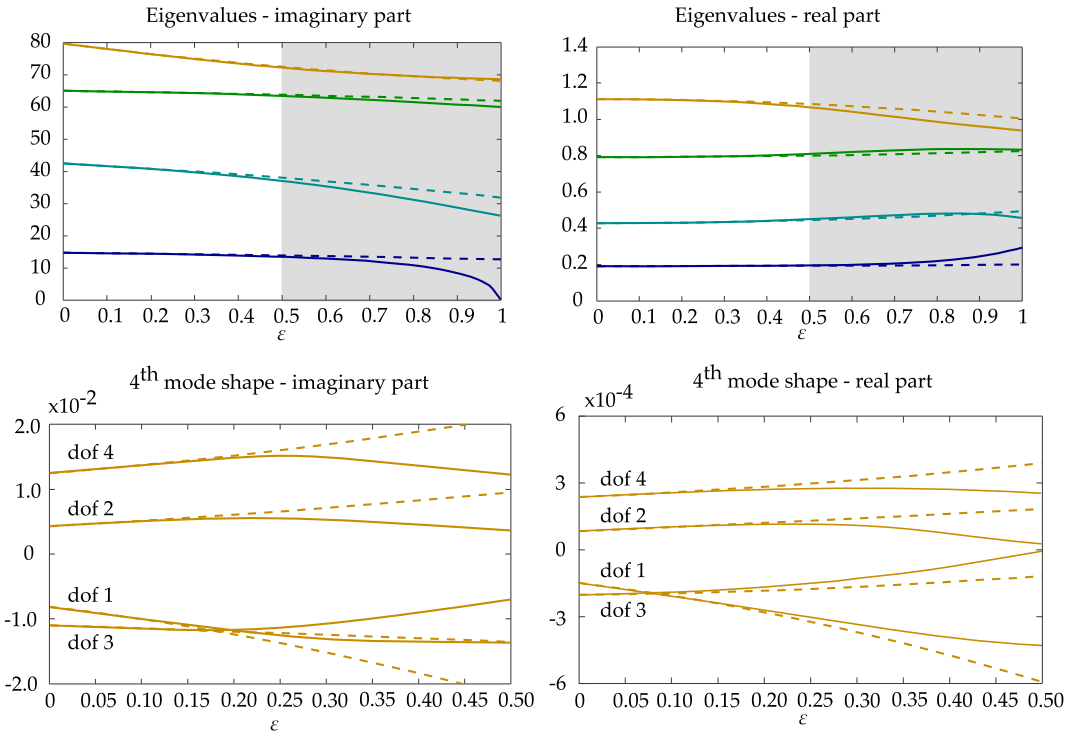

FIGURE 10 Complex eigensolutions (eigenvalues and fastest mode shape): case 1, second-order solution.

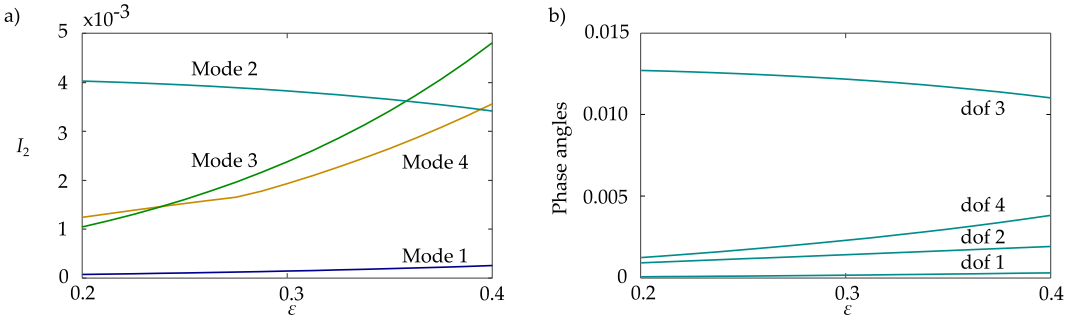

FIGURE 11 Index I_2: a) non increasing behaviour for the second mode and b) its explanation.

In the third damage case (a combination of decrease in stiffness and increase in damping), Figure 14 shows that the complexity index I_1 is not satisfying, since, apart from the usual first part (corresponding to very low values of the damage parameter), the curves do not exhibit monotonicity; moreover, approximated and actual curves cross each other, thus losing in reliability. Also the damage index I_3 appears to be inadequate for identification purpose, because its growth trend is not regular with the evolution of ε. On the other hand, the complexity indexes I_4 and I_5 look suitable to follow the increase in damage and the second-order approximated values meet the exact solution in a very satisfactory way: this is a key point in driving our identification procedure in what seems the most promising direction.

4.3 | Identification

Following the previous result on the reliability of modal complexity indexes for damage identification, the inverse problem of dynamics aimed at structural health monitoring is coped with by resorting to the second-order perturbation approach. We suppose we wish to monitor the health state of the benchmark structure of Figure 5, when it undergoes the three considered

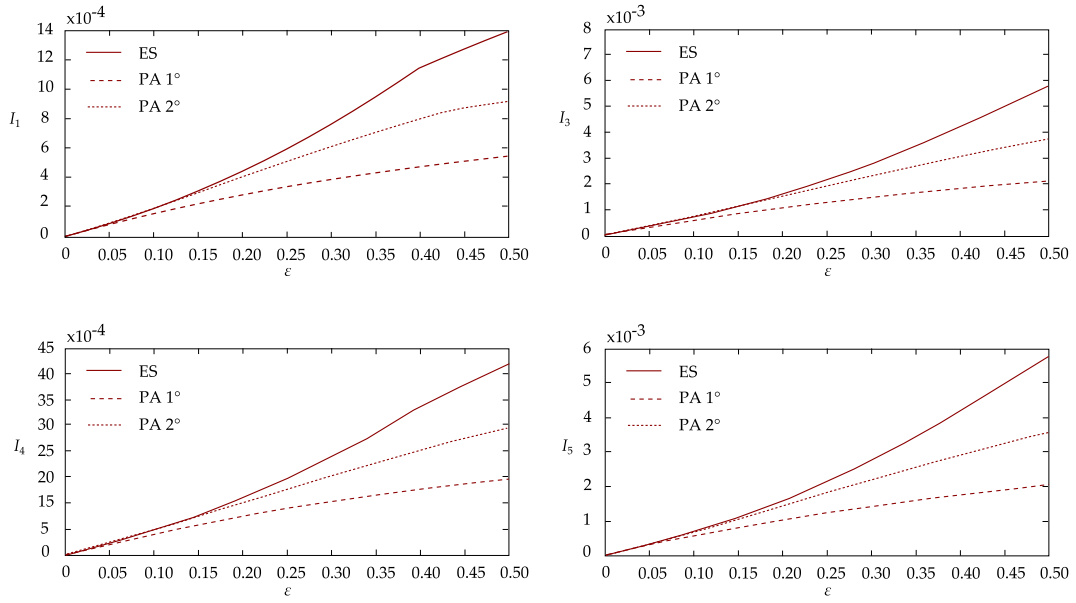

FIGURE 12 Complexity indexes for the damage case 1.

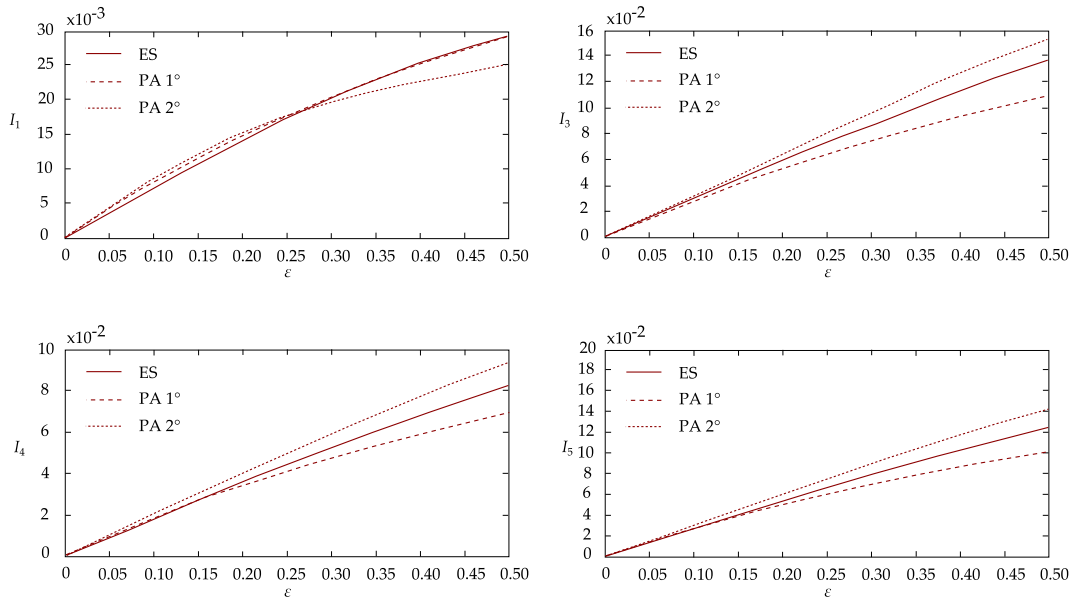

FIGURE 13 Complexity indexes for the damage case 2.

damage cases. With regard to identification, experimental quantities are here simulated numerically solving Eq. (9), where **M**, **C** and **K** are the mass, damping and stiffness matrices obtained by replacing the current value of the damage parameter ε.

Since we wish to numerically validate our approach for damage detection, we assume that $\mathbf{M}_0, \mathbf{C}_0, \mathbf{K}_0$ are exactly known from a previous experimental campaign (see the comments in Sub-section 3.2). Then, four different candidate models are adopted for the 4-story frame, each assuming that damage acts at a different floor as a linear variation of the relevant physical matrices (Figure 15). The results of damage identification are in Figures 16, 17, and 18 for the damage state 1, 2, 3, respectively. For all the cases our procedure properly selects the third candidate model of Figure 15, and the results are in a series of plots showing

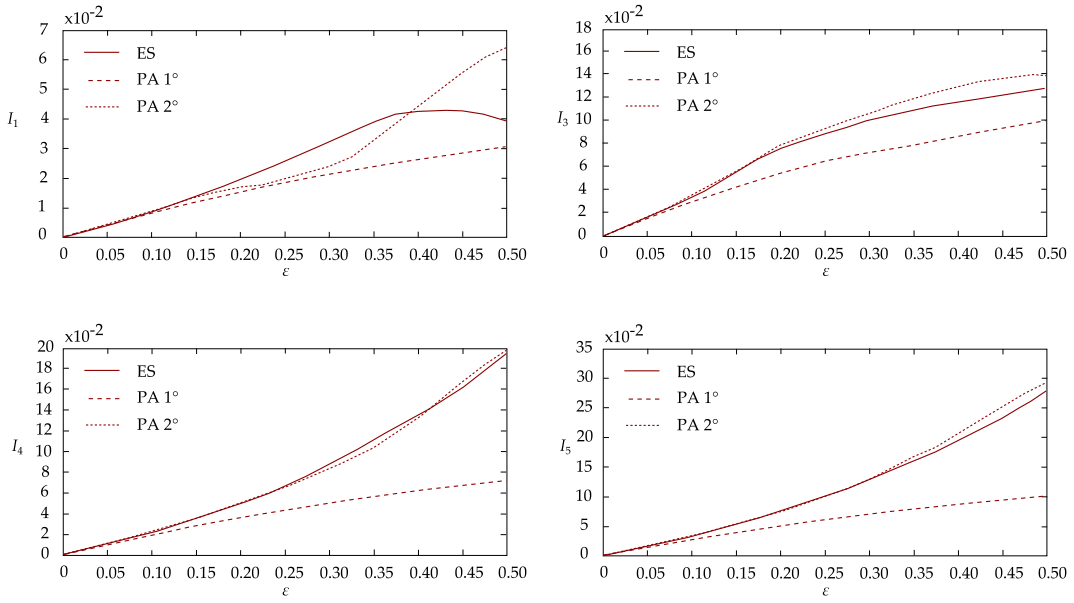

FIGURE 14 Complexity indexes for the damage case 3.

the identified parameter ε versus the actual one provided by the assumption on the damaged state; if identification were perfect, the two values should coincide, yielding the dashed line.

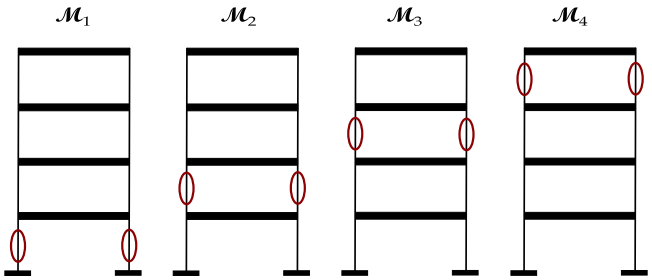

FIGURE 15 Sketch of selected candidate models.

Figure 16 shows that the identified damage parameter for this state is precise until a value $\varepsilon \approx 0.2$ (i.e., for a small evolution of damage from the initial condition), thus the identification is effective and accurate, regardless of the modal complexity index. However, when $\varepsilon > 0.2$ the discrepancies between the two lines cannot be neglected, and the identified parameter ε overestimates the actual amount of damage, which is in favour of safety, but not an optimum.

Figure 17 shows that the identified damage parameter for this state is again precise for very small values of ε, and identification is effective and accurate for all the I_h. After such values the discrepancies between the two lines are visible but not that remarkable; except for the index I_1, which does not exhibit a monotonic increase, the identified parameter ε underestimates the actual amount of damage.

Figure 18 shows that the identified damage evolution parameter for this damaged state is again accurate for small ε: identification is effective and accurate for all the modal complexity indexes. However, we see that the indexes I_4, I_5 have a very good identification performance for all the considered range of ε; since, in general, damage can actually be seen as both a reduction of stiffness and an increase of damping, the application of these two indexes in our identification procedure looks promising and effective.

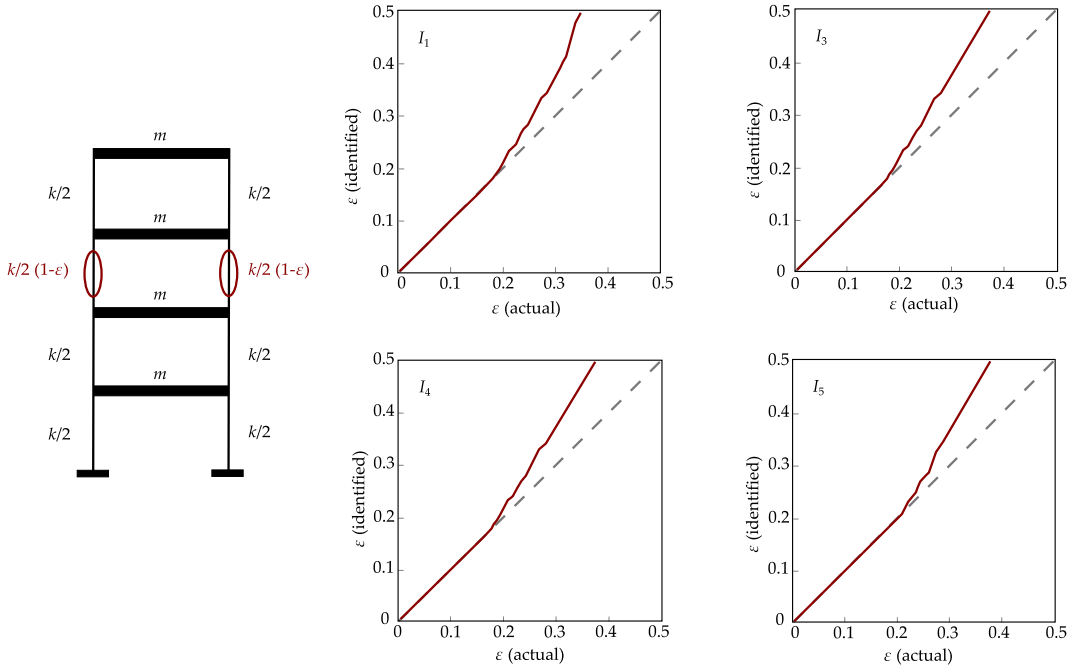

FIGURE 16 Damage identification results, case 1.

5 | FINAL REMARKS AND CONCLUSIONS

A perturbation approach relates damage to non-proportional damping, hence to natural mode shapes gaining an imaginary part, turning from real to complex. Damage dentification is based on the minima of an objective function comparing measured and analytical mode shapes; the latter are obtained by perturbing the initial undamaged system, i.e., damages are 'small' variations of healthy physical parameters.

A numerical validation considers three different damages: variation of stiffness, of damping, of both simultaneously. With the exception of the phase differences indicator (I_2), the other four non–negative scalar functions explored in this contribution prove to be effective to properly quantify local damages. Among these indexes, the average (I_4) and the weight (I_5) of the imaginary parts of the natural modes are the most reliable and stable in following damage evolution.

The inverse procedure ruled by the perturbation scheme is able to detect, locate and quantify damage in a wide range of the parameter ε with a low computational effort. In detail, a second-order approach shows negligible truncation errors when $\varepsilon \leq 0.20$, confirming our previous findings on adopting perturbation approaches in identification frames.

Ongoing studies are on experimental validations with noised signals; further developments focus on more general structures. Moreover, to improve the capability of the method in damage detection, the possibility to consider the overall eigensolution in the objective function is under investigation.

How to cite this article: Lofrano E., Paolone A., Ruta G.(2018), Dynamic damage identification using complex mode shapes, *Struct. Control Health Monit.*, *2018;00:1–1*.

APPENDIX

A PERTURBATION APPROACH

Vibration of non-proportionally damped discrete systems are ruled as described in Sub-section 2.2. By operating a perturbation technique, we are led to the eigenvalue problem in Eq. (22), which must be satisfied $\forall\varepsilon$. Thus, balancing equal powers of ε leads

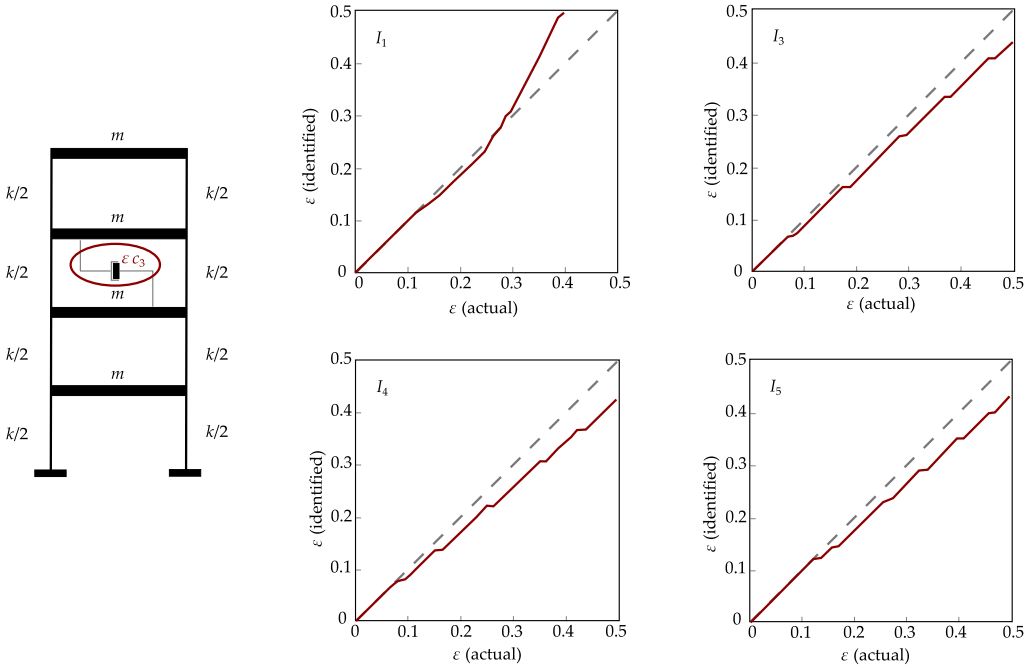

FIGURE 17 Damage identification results, case 2.

to a recursive list of $p+1$ sub-equations, with p the maximum power of ε in the expansion

$$\begin{aligned}
\varepsilon^0 &: (\mathbf{B}_0 - \lambda_{0i}\mathbf{A}_0)\mathbf{Z}_{0i} = \mathbf{0} \\
\varepsilon^1 &: (\mathbf{B}_0 - \lambda_{0i}\mathbf{A}_0)\mathbf{Z}_{1i} = (\lambda_{0i}\mathbf{A}_1 + \lambda_{1i}\mathbf{A}_0 - \mathbf{B}_1)\mathbf{Z}_{0i} \\
\varepsilon^2 &: (\mathbf{B}_0 - \lambda_{0i}\mathbf{A}_0)\mathbf{Z}_{2i} = (\lambda_{0i}\mathbf{A}_1 + \lambda_{1i}\mathbf{A}_0 - \mathbf{B}_1)\mathbf{Z}_{1i} + (\lambda_{0i}\mathbf{A}_2 + \lambda_{1i}\mathbf{A}_1 + \lambda_{2i}\mathbf{A}_0 - \mathbf{B}_2)\mathbf{Z}_{0i} \ \ldots
\end{aligned} \tag{A1}$$

We evaluate the first- and second-order terms of the eigenproperties $\lambda_i, \mathbf{Z}_i$ in the series expansion in Eq. (21).

A first-order solution follows the first-order expansion

$$\begin{cases} \mathbf{A} = \mathbf{A}_0 + \varepsilon\mathbf{A}_1 \\ \mathbf{B} = \mathbf{B}_0 + \varepsilon\mathbf{B}_1 \end{cases} \qquad \begin{cases} \lambda_i = \lambda_{0i} + \varepsilon\lambda_{1i} \\ \mathbf{Z}_i = \mathbf{Z}_{0i} + \varepsilon\mathbf{Z}_{1i} \end{cases} \tag{A2}$$

The *generating equation* (0-th order equation) provides the unperturbed terms $(\lambda_{0i}, \mathbf{Z}_{0i})$; then, the first-order correction is obtained by projecting $\mathbf{Z}_{1i}$ onto the $\mathbf{Z}_{0i}$ basis

$$\mathbf{Z}_{1i} = \sum_{j=1}^{2n} \mathbf{Z}_{0j}\alpha_{ij} \tag{A3}$$

Replacing Eq. (A3) into Eq. $(A1)_2$ yields

$$(\mathbf{B}_0 - \lambda_{0i}\mathbf{A}_0)\sum_{j=1}^{2n} \mathbf{Z}_{0j}\alpha_{ij} = (\lambda_{0i}\mathbf{A}_1 + \lambda_{1i}\mathbf{A}_0 - \mathbf{B}_1)\mathbf{Z}_{0i} \tag{A4}$$

and, pre-multiplying both sides by $\mathbf{Z}_{0i}^\top$

$$\mathbf{Z}_{0i}^\top(\mathbf{B}_0 - \lambda_{0i}\mathbf{A}_0)\sum_{j=1}^{2n} \mathbf{Z}_{0j}\alpha_{ij} = \mathbf{Z}_{0i}^\top(\lambda_{0i}\mathbf{A}_1 + \lambda_{1i}\mathbf{A}_0 - \mathbf{B}_1)\mathbf{Z}_{0i} \tag{A5}$$

whence, by orthogonality of the $\mathbf{Z}_{0j}$ with respect to $\mathbf{A}_0, \mathbf{B}_0$

$$\mathbf{Z}_{0i}^\top(\mathbf{B}_0 - \lambda_{0i}\mathbf{A}_0)\mathbf{Z}_{0i}\alpha_{ii} = \mathbf{Z}_{0i}^\top(\lambda_{0i}\mathbf{A}_1 + \lambda_{1i}\mathbf{A}_0 - \mathbf{B}_1)\mathbf{Z}_{0i} \tag{A6}$$

From the generating equation $(A1)_1$, the left-hand-side of Eq. (A6) vanishes, simplifying into

$$\mathbf{Z}_{0i}^\top(\lambda_{0i}\mathbf{A}_1 + \lambda_{1i}\mathbf{A}_0 - \mathbf{B}_1)\mathbf{Z}_{0i} = 0 \tag{A7}$$

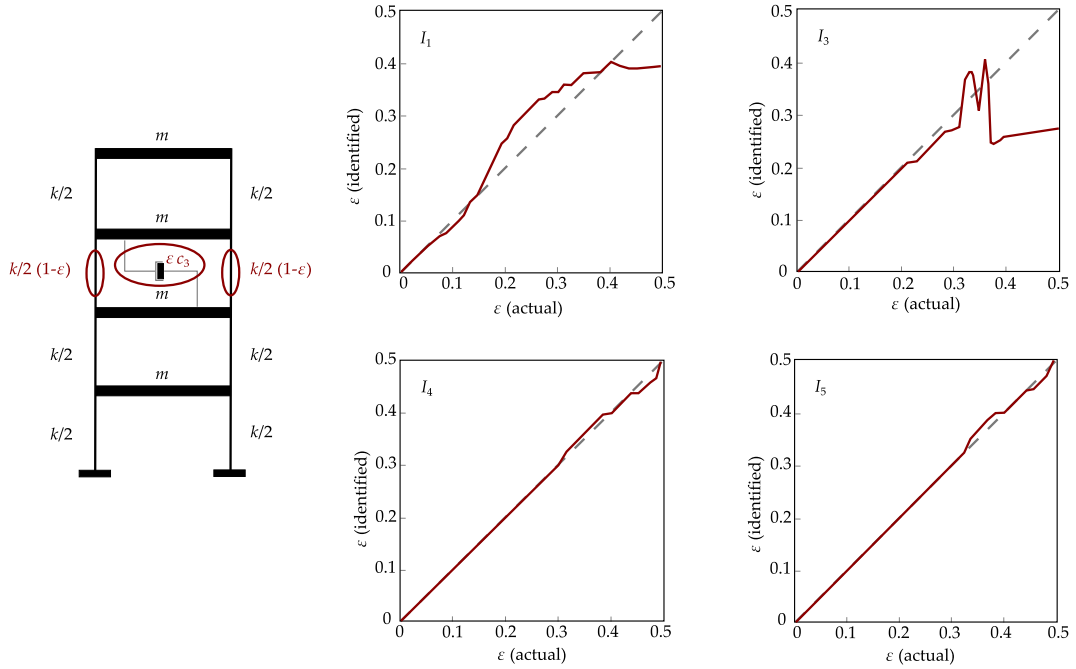

FIGURE 18 Damage identification results, case 3.

thus providing λ_{1i}

$$\lambda_{1i} = \frac{\mathbf{Z}_{0i}^{\top}(\mathbf{B}_1 - \lambda_{0i}\mathbf{A}_1)\mathbf{Z}_{0i}}{\mathbf{Z}_{0i}^{\top}\mathbf{A}_0\mathbf{Z}_{0i}} \tag{A8}$$

If both sides of Eq. (A4) are pre-multiplied by $\mathbf{Z}_{0k}^{\top}$, $k \neq i$

$$\mathbf{Z}_{0k}^{\top}(\mathbf{B}_0 - \lambda_{0i}\mathbf{A}_0)\sum_{j=1}^{2n}\mathbf{Z}_{0j}\alpha_{ij} = \mathbf{Z}_{0k}^{\top}(\lambda_{0i}\mathbf{A}_1 + \lambda_{1i}\mathbf{A}_0 - \mathbf{B}_1)\mathbf{Z}_{0i} \tag{A9}$$

The orthogonality of $\mathbf{Z}_{0j}$ with respect to $\mathbf{A}_0, \mathbf{B}_0$ yields

$$\mathbf{Z}_{0k}^{\top}(\mathbf{B}_0 - \lambda_{0i}\mathbf{A}_0)\mathbf{Z}_{0k}\alpha_{ik} = \mathbf{Z}_{0k}^{\top}(\lambda_{0i}\mathbf{A}_1 - \mathbf{B}_1)\mathbf{Z}_{0i} \tag{A10}$$

The generating equation $(A1)_1$ allows to replace $\mathbf{B}_0\mathbf{Z}_{0k}$ with $\lambda_{0k}\mathbf{A}_0\mathbf{Z}_{0k}$; then, Eq. (A10) becomes

$$\mathbf{Z}_{0k}^{\top}(\lambda_{0k} - \lambda_{0i})\mathbf{A}_0\mathbf{Z}_{0k}\alpha_{ik} = \mathbf{Z}_{0k}^{\top}(\lambda_{0i}\mathbf{A}_1 - \mathbf{B}_1)\mathbf{Z}_{0i} \tag{A11}$$

from which

$$\alpha_{ik} = \frac{\mathbf{Z}_{0k}^{\top}(\mathbf{B}_1 - \lambda_{0i}\mathbf{A}_1)\mathbf{Z}_{0i}}{(\lambda_{0i} - \lambda_{0k})\mathbf{Z}_{0k}^{\top}\mathbf{A}_0\mathbf{Z}_{0k}} \tag{A12}$$

Finally, by making - for convenience - a change of index

$$\alpha_{ij} = \frac{\mathbf{Z}_{0j}^{\top}(\mathbf{B}_1 - \lambda_{0i}\mathbf{A}_1)\mathbf{Z}_{0i}}{(\lambda_{0i} - \lambda_{0j})\mathbf{Z}_{0j}^{\top}\mathbf{A}_0\mathbf{Z}_{0j}} \tag{A13}$$

the eigenvectors $\mathbf{Z}_{1i}$ are obtained ruling Eq. (A3)

$$\mathbf{Z}_{1i} = \alpha_{ii}\mathbf{Z}_{0i} + \sum_{\substack{j=1 \\ j\neq i}}^{2n}\frac{\mathbf{Z}_{0j}^{\top}(\mathbf{B}_1 - \lambda_{0i}\mathbf{A}_1)\mathbf{Z}_{0i}}{(\lambda_{0i} - \lambda_{0j})\mathbf{Z}_{0j}^{\top}\mathbf{A}_0\mathbf{Z}_{0j}}\mathbf{Z}_{0j} \tag{A14}$$

where the coefficients $\alpha_{ii} \in \mathbb{R}$ are indeterminate and play the role of multiplicative constants.

A second-order solution follows the expansions

$$\begin{cases} \mathbf{A} = \mathbf{A}_0 + \varepsilon\mathbf{A}_1 + \varepsilon^2\mathbf{A}_2 \\ \mathbf{B} = \mathbf{B}_0 + \varepsilon\mathbf{B}_1 + \varepsilon^2\mathbf{B}_2 \end{cases} \quad \begin{cases} \lambda_i = \lambda_{0i} + \varepsilon\lambda_{1i} + \varepsilon^2\lambda_{2i} \\ \mathbf{Z}_i = \mathbf{Z}_{0i} + \varepsilon\mathbf{Z}_{1i} + \varepsilon^2\mathbf{Z}_{2i} \end{cases} \tag{A15}$$

where the 0-th and 1-st order solutions are assumed known. Then, the eigenvector $\mathbf{Z}_{2i}$ is projected onto the $\mathbf{Z}_{0i}$

$$\mathbf{Z}_{2i} = \sum_{j=1}^{2n} \mathbf{Z}_{0j}\beta_{ij} \tag{A16}$$

Replacing such projection into the second-order eigenvalue problem Eq. $(A1)_3$ yields

$$(\mathbf{B}_0 - \lambda_{0i}\mathbf{A}_0)\sum_{j=1}^{2n} \mathbf{Z}_{0j}\beta_{ij} = (\lambda_{0i}\mathbf{A}_1 + \lambda_{1i}\mathbf{A}_0 - \mathbf{B}_1)\mathbf{Z}_{1i} + (\lambda_{0i}\mathbf{A}_2 + \lambda_{1i}\mathbf{A}_1 + \lambda_{2i}\mathbf{A}_0 - \mathbf{B}_2)\mathbf{Z}_{0i} \tag{A17}$$

Premultiplying both sides of Eq. (A17) by $\mathbf{Z}_{0i}^\top$ yields

$$\mathbf{Z}_{0i}^\top(\mathbf{B}_0 - \lambda_{0i}\mathbf{A}_0)\sum_{j=1}^{2n} \mathbf{Z}_{0j}\beta_{ij} = \mathbf{Z}_{0i}^\top(\lambda_{0i}\mathbf{A}_1 + \lambda_{1i}\mathbf{A}_0 - \mathbf{B}_1)\mathbf{Z}_{1i} + \mathbf{Z}_{0i}^\top(\lambda_{0i}\mathbf{A}_2 + \lambda_{1i}\mathbf{A}_1 + \lambda_{2i}\mathbf{A}_0 - \mathbf{B}_2)\mathbf{Z}_{0i} \tag{A18}$$

whence, by orthogonality of the $\mathbf{Z}_{0j}$ with respect to $\mathbf{A}_0, \mathbf{B}_0$

$$\mathbf{Z}_{0i}^\top(\mathbf{B}_0 - \lambda_{0i}\mathbf{A}_0)\mathbf{Z}_{0i}\beta_{ii} = \mathbf{Z}_{0i}^\top(\lambda_{0i}\mathbf{A}_1 + \lambda_{1i}\mathbf{A}_0 - \mathbf{B}_1)\mathbf{Z}_{1i} + \mathbf{Z}_{0i}^\top(\lambda_{0i}\mathbf{A}_2 + \lambda_{1i}\mathbf{A}_1 + \lambda_{2i}\mathbf{A}_0 - \mathbf{B}_2)\mathbf{Z}_{0i} \tag{A19}$$

From the generating equation $(A1)_1$, the left-hand-side of Eq. (A19) vanishes, simplifying into

$$\mathbf{Z}_{0i}^\top(\lambda_{0i}\mathbf{A}_1 + \lambda_{1i}\mathbf{A}_0 - \mathbf{B}_1)\mathbf{Z}_{1i} + \mathbf{Z}_{0i}^\top(\lambda_{0i}\mathbf{A}_2 + \lambda_{1i}\mathbf{A}_1 + \lambda_{2i}\mathbf{A}_0 - \mathbf{B}_2)\mathbf{Z}_{0i} = 0 \tag{A20}$$

thus providing λ_{2i}

$$\lambda_{2i} = \frac{\mathbf{Z}_{0i}^\top(\mathbf{B}_1 - \lambda_{0i}\mathbf{A}_1 - \lambda_{1i}\mathbf{A}_0)\mathbf{Z}_{1i}}{\mathbf{Z}_{0i}^\top\mathbf{A}_0\mathbf{Z}_{0i}} + \frac{\mathbf{Z}_{0i}^\top(\mathbf{B}_2 - \lambda_{0i}\mathbf{A}_2 - \lambda_{1i}\mathbf{A}_1)\mathbf{Z}_{0i}}{\mathbf{Z}_{0i}^\top\mathbf{A}_0\mathbf{Z}_{0i}} \tag{A21}$$

If both sides of Eq. (A17) are pre-multiplied by $\mathbf{Z}_{0k}^\top, k \neq i$

$$\mathbf{Z}_{0k}^\top(\mathbf{B}_0 - \lambda_{0i}\mathbf{A}_0)\sum_{j=1}^{2n} \mathbf{Z}_{0j}\beta_{ij} = \mathbf{Z}_{0k}^\top(\lambda_{0i}\mathbf{A}_1 + \lambda_{1i}\mathbf{A}_0 - \mathbf{B}_1)\mathbf{Z}_{1i} + \mathbf{Z}_{0k}^\top(\lambda_{0i}\mathbf{A}_2 + \lambda_{1i}\mathbf{A}_1 + \lambda_{2i}\mathbf{A}_0 - \mathbf{B}_2)\mathbf{Z}_{0i} \tag{A22}$$

The orthogonality of $\mathbf{Z}_{0j}$ with respect to $\mathbf{A}_0, \mathbf{B}_0$ yields

$$\mathbf{Z}_{0k}^\top(\mathbf{B}_0 - \lambda_{0i}\mathbf{A}_0)\mathbf{Z}_{0k}\beta_{ik} = \mathbf{Z}_{0k}^\top(\lambda_{0i}\mathbf{A}_1 + \lambda_{1i}\mathbf{A}_0 - \mathbf{B}_1)\mathbf{Z}_{1i} + \mathbf{Z}_{0k}^\top(\lambda_{0i}\mathbf{A}_2 + \lambda_{1i}\mathbf{A}_1 - \mathbf{B}_2)\mathbf{Z}_{0i} \tag{A23}$$

The generating equation $(A1)_1$ allows to replace $\mathbf{B}_0\mathbf{Z}_{0k}$ with $\lambda_{0k}\mathbf{A}_0\mathbf{Z}_{0k}$; then, Eq. (A23) becomes

$$\mathbf{Z}_{0k}^\top(\lambda_{0k} - \lambda_{0i})\mathbf{A}_0\mathbf{Z}_{0k}\beta_{ik} = \mathbf{Z}_{0k}^\top(\lambda_{0i}\mathbf{A}_1 + \lambda_{1i}\mathbf{A}_0 - \mathbf{B}_1)\mathbf{Z}_{1i} + \mathbf{Z}_{0k}^\top(\lambda_{0i}\mathbf{A}_2 + \lambda_{1i}\mathbf{A}_1 - \mathbf{B}_2)\mathbf{Z}_{0i} \tag{A24}$$

from which

$$\beta_{ik} = \frac{\mathbf{Z}_{0k}^\top(\mathbf{B}_1 - \lambda_{0i}\mathbf{A}_1 - \lambda_{1i}\mathbf{A}_0)\mathbf{Z}_{1i}}{(\lambda_{0i} - \lambda_{0k})\mathbf{Z}_{0k}^\top\mathbf{A}_0\mathbf{Z}_{0k}} + \frac{\mathbf{Z}_{0k}^\top(\mathbf{B}_2 - \lambda_{0i}\mathbf{A}_2 - \lambda_{1i}\mathbf{A}_1)\mathbf{Z}_{0i}}{(\lambda_{0i} - \lambda_{0k})\mathbf{Z}_{0k}^\top\mathbf{A}_0\mathbf{Z}_{0k}} \tag{A25}$$

Finally, by making - for convenience - a change of index

$$\beta_{ij} = \frac{\mathbf{Z}_{0j}^\top(\mathbf{B}_1 - \lambda_{0i}\mathbf{A}_1 - \lambda_{1i}\mathbf{A}_0)\mathbf{Z}_{1i}}{(\lambda_{0i} - \lambda_{0j})\mathbf{Z}_{0j}^\top\mathbf{A}_0\mathbf{Z}_{0j}} + \frac{\mathbf{Z}_{0j}^\top(\mathbf{B}_2 - \lambda_{0i}\mathbf{A}_2 - \lambda_{1i}\mathbf{A}_1)\mathbf{Z}_{0i}}{(\lambda_{0i} - \lambda_{0j})\mathbf{Z}_{0j}^\top\mathbf{A}_0\mathbf{Z}_{0j}} \tag{A26}$$

the eigenvectors $\mathbf{Z}_{2i}$ are obtained ruling Eq. (A16)

$$\mathbf{Z}_{2i} = \beta_{ii}\mathbf{Z}_{0i} + \sum_{\substack{j=1 \\ j\neq i}}^{2n} \left(\frac{\mathbf{Z}_{0j}^\top(\mathbf{B}_1 - \lambda_{0i}\mathbf{A}_1 - \lambda_{1i}\mathbf{A}_0)\mathbf{Z}_{1i}}{(\lambda_{0i} - \lambda_{0j})\mathbf{Z}_{0j}^\top\mathbf{A}_0\mathbf{Z}_{0j}} + \frac{\mathbf{Z}_{0j}^\top(\mathbf{B}_2 - \lambda_{0i}\mathbf{A}_2 - \lambda_{1i}\mathbf{A}_1)\mathbf{Z}_{0i}}{(\lambda_{0i} - \lambda_{0j})\mathbf{Z}_{0j}^\top\mathbf{A}_0\mathbf{Z}_{0j}} \right)\mathbf{Z}_{0j} \tag{A27}$$

where the $\beta_{ii} \in \mathbb{R}$ coefficients remain indeterminate and play the role of the generic multiplicative constants.

Thus, if $\left(\alpha_{ii}, \beta_{ii}\right) \in \mathbb{R}$, a second-order perturbation approach provides the eigenpairs $\lambda_i, \mathbf{Z}_i$

$$\begin{cases} \lambda_{1i} = \dfrac{\mathbf{Z}_{0i}^{\top}(\mathbf{B}_1 - \lambda_{0i}\mathbf{A}_1)\mathbf{Z}_{0i}}{\mathbf{Z}_{0i}^{\top}\mathbf{A}_0\mathbf{Z}_{0i}} \\ \mathbf{Z}_{1i} = \alpha_{ii}\mathbf{Z}_{0i} + \displaystyle\sum_{\substack{j=1 \\ j\neq i}}^{2n} \frac{\mathbf{Z}_{0j}^{\top}(\mathbf{B}_1 - \lambda_{0i}\mathbf{A}_1)\mathbf{Z}_{0i}}{(\lambda_{0i} - \lambda_{0j})\mathbf{Z}_{0j}^{\top}\mathbf{A}_0\mathbf{Z}_{0j}}\mathbf{Z}_{0j} \end{cases} \tag{A28}$$

$$\begin{cases} \lambda_{2i} = \dfrac{\mathbf{Z}_{0i}^{\top}(\mathbf{B}_1 - \lambda_{0i}\mathbf{A}_1 - \lambda_{1i}\mathbf{A}_0)\mathbf{Z}_{1i}}{\mathbf{Z}_{0i}^{\top}\mathbf{A}_0\mathbf{Z}_{0i}} + \dfrac{\mathbf{Z}_{0i}^{\top}(\mathbf{B}_2 - \lambda_{0i}\mathbf{A}_2 - \lambda_{1i}\mathbf{A}_1)\mathbf{Z}_{0i}}{\mathbf{Z}_{0i}^{\top}\mathbf{A}_0\mathbf{Z}_{0i}} \\ \mathbf{Z}_{2i} = \beta_{ii}\mathbf{Z}_{0i} + \sum_{\substack{j=1 \\ j\neq i}}^{2n} \left(\dfrac{\mathbf{Z}_{0j}^{\top}(\mathbf{B}_1 - \lambda_{0i}\mathbf{A}_1 - \lambda_{1i}\mathbf{A}_0)\mathbf{Z}_{1i}}{(\lambda_{0i} - \lambda_{0j})\mathbf{Z}_{0j}^{\top}\mathbf{A}_0\mathbf{Z}_{0j}} + \dfrac{\mathbf{Z}_{0j}^{\top}(\mathbf{B}_2 - \lambda_{0i}\mathbf{A}_2 - \lambda_{1i}\mathbf{A}_1)\mathbf{Z}_{0i}}{(\lambda_{0i} - \lambda_{0j})\mathbf{Z}_{0j}^{\top}\mathbf{A}_0\mathbf{Z}_{0j}} \right)\mathbf{Z}_{0j} \end{cases}$$

References

1. Doebling S, Farrar CR, Prime M and Shevitz D (1996) *Damage identification and health monitoring of structural and mechanical systems from changes in their vibration characteristics: a literature review*, Los Alamos National Laboratory Report LA-13070-MS.

2. Farrar CR, Doebling S and Nix D (2001) *Vibration-based structural damage identification*, Phil. Trans. Royal Society A, 359(1778), 131.

3. Peeters B, Maeck J and Roeck GD (2001) *Vibration-based damage detection in civil engineering: excitation sources and temperature effects*, Smart Materials and Structures 10:518–527.

4. Farrar CR and Worden K ed. (2007) *Structural Health Monitoring*, theme issue, Phil. Trans. Royal Society A, 365(1851).

5. Balageas D, Fritzen CP and Güemes A ed. (2006) *Structural Health Monitoring*, ISTE, London.

6. Farrar CR and Worden K ed. (2013) *Structural Health Monitoring: A Machine Learning Perspective*, J. Wiley & Sons, New York.

7. Morassi A and Vestroni F ed. (2008) *Dynamic Methods for Damage Detection in Structures*, CISM International Centre for Mechanical Sciences, Springer-Verlag, Wien.

8. Cawley P and Adams RD (1979) *The location of defects in structures from measurements of natural frequencies*, Journal of Strain Analysis 14:49–57.

9. Christides S and Barr ADS (1984) *One-dimensional theory of cracked Bernoulli-Euler beams*, International Journal of Mechanical Sciences 26:639–648.

10. Gladwell GML (1984) *The inverse problem for the vibrating beams*, Proceedings of the Royal Society of London A 393:277–295.

11. Liang RY, Choy F and Hu J (1990) *Identification of cracks in beam structure using measurements of natural frequencies*, Journal of Franklin Institute 324:505–518.

12. Liang RY, Hu J and Choy F (1992) *Quantitative NDE technique for assessing damages in beam structures*, Journal of Engineering Mechanics 118:1469–1487.

13. Vestroni F and Capecchi D (2000) *Damage detection in beams structures based on frequency measurements*, Journal of Engineering Mechanics 126:761–768.

14. Sinha JK, Friswell MI and Edwards S (2002) *Simplified models for the location of cracks in beam structures using measured vibration data*, Journal of Sound and Vibration 251:13–38.

15. Cerri MN and Ruta G (2004) *Detection of localised damage in plane circular arches by frequency data*, Journal of Sound and Vibration 270:39–59.

16. Cerri MN, Dilena M and Ruta G (2008) *Vibration and damage detection in undamaged and cracked circular arches: Experimental and analytical results*, Journal of Sound and Vibration 314:83–94.

17. Lofrano E, Paolone A and Romeo F (2014) *Damage identification in a parabolic arch through the combined use of modal properties and empirical mode decomposition*, Proceedings of the International Conference on Structural Dynamic EuroDyn:2643–2650.

18. Loh CH, Loh KJ, Yang YS, Hsiung WY, and Huang YT (2017) *Vibration-based system identification of wind turbine system*, Struct. Control Health Monit. 24:e1876.

19. Rainieri C, Fabbrocino G and Cosenza E (2011) *Integrated seismic early warning and structural health monitoring of critical civil infrastructures in seismically prone areas*, Structural Health Monitoring 10:291-308.

20. Oregui M, Li S, Núñez A, Li Z, Carroll R, and Dollevoet R (2017) *Monitoring bolt tightness of rail joints using axle box acceleration measurements*, Struct. Control Health Monit. 24:e1848.

21. Diaferio M and Sepe V (2016) *Modal identification of damaged frames*, Struct. Control Health Monit. 23:82–102.

22. Antonacci E, De Stefano A, Gattulli V, Lepidi M and Matta E (2012) *Comparative study of vibration-based parametric identification techniques for a three-dimensional frame structure*, Struct. Control Health Monit. 19:579–608.

23. Ong WH, Chiu WK, Russ M and Chiu ZK (2016) *Integrating sensing elements on external fixators for healing assessment of fractured femur*, Struct. Control Health Monit. 23:1388–1404.

24. Chopra AK (1980) *Dinamycs of Structures*, Earthquake Engineering Research Institute, Berkeley, 1980.

25. Craig RR and Kurdila RJ (2006) *Fundamentals of Structural Dynamics* 2nd ed., J. Wiley & Sons, New York.

26. Kawiecki G (2001) *Modal damping measurement for damage detection*, Smart Materials and Structures 10:466–471.

27. Iezzi F, Spina D and Valente C (2015) *Damage assessment through changes in mode shapes due to non-proportional damping*, Journal of Physics: Conference Series 628:012019.

28. Link M, Boettcher T and Zhang L (2006) *Computational Model Updating of Structures with Non-Proportional Damping*, Proceedings of the 24th International Modal Analysis Conference, Sant Louis, Missouri.

29. Lofrano E, Paolone A, Ruta G and Taglioni A (2017) *Perturbation damage indicators based on complex modes*, Procedia Engineering 199:1949–1954.

30. Caughey TK and O'Kelly MEJ (1965) *Classical normal modes in damped linear dynamic systems*, Transactions of ASME, Journal of Applied Mechanics 32:583–588.

31. Liu K and Zheng W (2000) *Quantification of non-proportionality of damping in discrete vibratory systems*, Computers and Structures 77:557–570.

32. Ewins DJ (2000) *Modal Testing: Theory, Practice and Applications*, 2nd ed., J. Wiley & Sons, New York.

33. Imregun M and Ewins DJ (1995) *Complex modes - origin and limits*, Proceedings of the 13th International Modal Analysis Conference, Nashville, Tennessee.

34. Cabboi A, Magalhães F, Gentile C and Cunha Á (2017) *Automated modal identification and tracking: Application to an iron arch bridge*, Struct. Control Health Monit. 24(1):e1854/1–20.

35. Ibrahim RS and Sestieri Aldo (1995) *Existence and Normalization of Complex Modes in Post Experimental Use in Modal Analysis*,, Proceedings of the 13th International Modal Analysis Conference, Nashville, Tennessee.

36. Alderucci T and Muscolino G (2017) *Time-frequency varying response functions of non-classically damped linear structures under fully non-stationary stochastic excitations*, Probabilistic Engineering Mechanics, article in press, http://dx.doi.org/10.1016/j.probengmech.2017.08.004.

37. Prater G and Singh R (1985) *Quantification of the extent of non proportional viscous damping in discrete vibratory systems*, Journal of Sound and Vibration 104:109–125.

38. Valente C, Spina D, Gabriele S and De Leonardis A (2010) *The complex plane representation method for structural damage detection*, Proceedings of the 10th International Conference on Computational Structures Technology.

39. Lofrano E, Paolone A and Vasta M (2016) *A perturbation approach for the identification of uncertain structures*, International Journal of Dynamics and Control 4:204–212.

40. Lofrano E, Paolone A and Vasta M (2016) *Dynamic identification of classically damped uncertain structures*, Conference Proceedings of the Society for Experimental Mechanics Series 3:131–142.

41. Pignataro M and Ruta G (2003) *Coupled instabilities in thin-walled beams: a qualitative approach*, European Journal of Mechanics A: Solids 22:139–149.

42. Ruta G, Varano V, Pignataro M and Rizzi N (2008) *A beam model for the flexural-torsional buckling of thin-walled members with some applications*, Thin-Walled Structures 46:816–822.

43. dell'Isola F, Ruta G and Batra RC (1998) *Generalized Poynting effects in pre-deformed prismatic bars*, Journal of Elasticity 50:181–196.

44. Batra RC, dell'Isola F and Ruta G (2005) *Second-order solution of Saint-Venant's problem for an elastic bar pre-deformed in flexure*, International Journal of Non-Linear Mechanics 40:411-422.

45. Nayfeh AH (1973) *Perturbation methods*, J. Wiley & Sons, New York.

46. Lacarbonara W, Arena A and Antman SS (2015) *Flexural vibrations of nonlinearly elastic circular rings*, Meccanica 50(3):689–705.

47. Lofrano E, Paolone A and Vasta M (2016) *Identification of uncertain vibrating beams through a perturbation approach*, ASCE-ASME Journal of Risk and Uncertainty in Engineering Systems, Part A: Civil Engineering 2(2):C4015006/1–12.

48. Kato T (1980) *Perturbation Theory for Linear Operators*, corrected printing 2nd ed., Springer-Verlag, Berlin Heidelberg New York.

49. Luongo A, Paolone A and Di Egidio A, *Sensitivities and Linear Stability Analysis Around a Double-Zero Eigenvalue*, AIAA Journal 38(4):702–710.

50. Lepidi M (2013) *Multi-parameter perturbation methods for the eigensolution sensitivity analysis of nearly-resonant non-defective multi-degree-of-freedom systems*, Journal of Sound and Vibration 332(4):1011–1032.

51. Allemang RJ and Brown DL (1982) *A correlation coefficient for modal vector analysis*, 1st International Modal Analysis Conference.

52. Allemang RJ (2003) *The Modal Assurance Criterion (MAC): twenty years of use and abuse*, Sound and Vibration Magazine, 37(8):14–23.

53. Rytter T (1993) *Vibration based inspection of civil engineering structure*, PhD dissertation, Department of building technology and structure engineering, Aalborg University, Denmark.

54. Worden K, Farrar CR, Manson Gand and Park G (2007) *The fundamental axioms of structural health monitoring*, Proceedings of the Royal Society of London A 463(2082):1639–1664.

55. Olsen P, Skafte A, Hansen JB, Hovgaard MK, Brincker R and Ventura C (2013) *Identification of systems with complex modes using OMA*, 5th International Operational Modal Analysis Conference.